

- van der Stok M, Nair K, Khan N, Crawford H, Payne R, Leslie A, Prado J, Prendergast A, Frater J, McCarthy N, Brander C, Learn GH, Nickle D, Rousseau C, Coovadia H, Mullins JI, Heckerman D, Walker BD, Goulder P. 2007. CD8⁺ T-cell responses to different HIV proteins have discordant associations with viral load. *Nat. Med.* 13:46–53. <http://dx.doi.org/10.1038/nm1520>.
17. Migueles SA, Sabbaghian MS, Shupert WL, Bettinotti MP, Marincola FM, Martino L, Hallahan CW, Selig SM, Schwartz D, Sullivan J, Connors R. 2000. HLA B*5701 is highly associated with restriction of virus replication in a subgroup of HIV-infected long term nonprogressors. *Proc. Natl. Acad. Sci. U. S. A.* 97:2709–2714. <http://dx.doi.org/10.1073/pnas.050567397>.
 18. Mühl T, Krawczak M, Ten Haaf P, Hunsmann G, Sauermann U. 2002. MHC class I alleles influence set-point viral load and survival time in simian immunodeficiency virus-infected rhesus monkeys. *J. Immunol.* 169:3438–3446.
 19. Tang J, Tang S, Lobashevsky E, Myracle AD, Fideli U, Aldrovandi G, Allen S, Musonda R, Kaslow RA, Zambia-UAB HIV Research Project. 2002. Favorable and unfavorable HLA class I alleles and haplotypes in Zambians predominantly infected with clade C human immunodeficiency virus type 1. *J. Virol.* 76:8276–8284. <http://dx.doi.org/10.1128/JVI.76.16.8276-8284.2002>.
 20. Altfeld M, Addo MM, Rosenberg ES, Hecht FM, Lee PK, Vogel M, Yu XG, Draenert R, Johnston MN, Strick D, Allen TM, Feeney ME, Kahn JO, Sekaly RP, Levy JA, Rockstroh JK, Goulder PJ, Walker BD. 2003. Influence of HLA-B57 on clinical presentation and viral control during acute HIV-1 infection. *AIDS* 17:2581–2591. <http://dx.doi.org/10.1097/00002030-200312050-00005>.
 21. Kiepiela P, Leslie AJ, Honeyborne I, Ramduth D, Thobakgale C, Chetty S, Rathnavalu P, Moore C, Pfafferott KJ, Hilton L, Zimbwa P, Moore S, Allen T, Brander C, Addo MM, Altfeld M, James I, Mallal S, Bunce M, Barber LD, Szinger J, Day C, Klenerman P, Mullins J, Korber B, Coovadia HM, Walker BD, Goulder PJ. 2004. Dominant influence of HLA-B in mediating the potential co-evolution of HIV and HLA. *Nature* 432:769–775. <http://dx.doi.org/10.1038/nature03113>.
 22. Bontrop RE, Watkins DI. 2005. MHC polymorphism: AIDS susceptibility in nonhuman primates. *Trends Immunol.* 26:227–233. <http://dx.doi.org/10.1016/j.it.2005.02.003>.
 23. Yant LJ, Friedrich TC, Johnson RC, May GE, Maness NJ, Enz AM, Lifson JD, O'Connor DH, Carrington M, Watkins DI. 2006. The high-frequency major histocompatibility complex class I allele Mamu-B*17 is associated with control of simian immunodeficiency virus SIVmac239 replication. *J. Virol.* 80:5074–5077. <http://dx.doi.org/10.1128/JVI.80.10.5074-5077.2006>.
 24. Loffredo JT, Maxwell J, Qi Y, Glidden CE, Borchardt GJ, Soma T, Bean AT, Beal DR, Wilson NA, Rehauer WM, Lifson JD, Carrington M, Watkins DI. 2007. Mamu-B*08-positive macaques control simian immunodeficiency virus replication. *J. Virol.* 81:8827–8832. <http://dx.doi.org/10.1128/JVI.00895-07>.
 25. Takahashi N, Nomura T, Takahara Y, Yamamoto H, Shiino T, Takeda A, Inoue M, Iida A, Hara H, Shu T, Hasegawa M, Sakawaki H, Miura T, Igarashi T, Koyanagi Y, Naruse TK, Kimura A, Matano T. 2013. A novel protective MHC-I haplotype not associated with dominant Gag-specific CD8⁺ T-cell responses in SIVmac239 infection of Burmese rhesus macaques. *PLoS One* 8:e54300. <http://dx.doi.org/10.1371/journal.pone.0054300>.
 26. Friedrich TC, Dodds EJ, Yant LJ, Vojnov L, Rudersdorf R, Cullen C, Evans DT, Desrosiers RC, Mothé BR, Sidney J, Sette A, Kunstman K, Wolinsky S, Piatak M, Lifson J, Hughes AL, Wilson N, O'Connor DH, Watkins DI. 2004. Reversion of CTL escape-variant immunodeficiency viruses in vivo. *Nat. Med.* 10:275–281. <http://dx.doi.org/10.1038/nm998>.
 27. Leslie AJ, Pfafferott KJ, Chetty P, Draenert R, Addo MM, Feeney M, Tang Y, Holmes EC, Allen T, Prado JG, Altfeld M, Brander C, Dixon C, Ramduth D, Jeena P, Thomas SA, St John A, Roach TA, Kupfer B, Luzzi G, Edwards A, Taylor G, Lyall H, Tudor-Williams G, Novelli V, Martinez-Picado J, Kiepiela P, Walker BD, Goulder PJ. 2004. HIV evolution: CTL escape mutation and reversion after transmission. *Nat. Med.* 10:282–289. <http://dx.doi.org/10.1038/nm992>.
 28. Feeney ME, Tang Y, Roosevelt KA, Leslie AJ, McIntosh K, Karthas N, Walker BD, Goulder PJ. 2004. Immune escape precedes breakthrough human immunodeficiency virus type 1 viremia and broadening of the cytotoxic T-lymphocyte response in an HLA-B27-positive long-term-nonprogressing child. *J. Virol.* 78:8927–8930. <http://dx.doi.org/10.1128/JVI.78.16.8927-8930.2004>.
 29. Goulder PJR, Watkins DI. 2008. Impact of MHC class I diversity on immune control of immunodeficiency virus replication. *Nat. Rev. Immunol.* 8:619–630. <http://dx.doi.org/10.1038/nri2357>.
 30. Goulder PJR, Watkins DI. 2004. HIV and SIV CTL escape: implications for vaccine design. *Nat. Rev. Immunol.* 4:630–640. <http://dx.doi.org/10.1038/nri1417>.
 31. Martinez-Picado J, Prado JG, Fry EE, Pfafferott K, Leslie A, Chetty S, Thobakgale C, Honeyborne I, Crawford H, Matthews P, Pillay T, Rousseau C, Mullins JI, Brander C, Walker BD, Stuart DI, Kiepiela P, Goulder P. 2006. Fitness cost of escape mutations in p24 Gag in association with control of human immunodeficiency virus type 1. *J. Virol.* 80:3617–3623. <http://dx.doi.org/10.1128/JVI.80.7.3617-3623.2006>.
 32. Schneidewind A, Brockman MA, Yang R, Adam RI, Li B, Le Gall S, Rinaldo CR, Craggs SL, Allgaier RL, Power KA, Kuntzen T, Tung CS, LaBute MX, Mueller SM, Harrer T, McMichael AJ, Goulder PJ, Aiken C, Brander C, Kelleher AD, Allen TM. 2007. Escape from the dominant HLA-B27-restricted cytotoxic T-lymphocyte response in Gag is associated with a dramatic reduction in human immunodeficiency virus type 1 replication. *J. Virol.* 81:12382–12393. <http://dx.doi.org/10.1128/JVI.01543-07>.
 33. Miura T, Brockman MA, Schneidewind A, Lobritz M, Pereyra F, Rathod A, Block BL, Brumme ZL, Brumme CJ, Baker B, Rothchild AC, Li B, Trocha A, Cutrell E, Frahm N, Brander C, Toth I, Arts EJ, Allen TM, Walker BD. 2009. HLA-B57/B*5801 human immunodeficiency virus type 1 elite controllers select for rare gag variants associated with reduced viral replication capacity and strong cytotoxic T-lymphocyte recognition. *J. Virol.* 83:2743–2755. <http://dx.doi.org/10.1128/JVI.02265-08>.
 34. Loffredo JT, Bean AT, Beal DR, León EJ, May GE, Piskowski SM, Furlott JR, Reed J, Musani SK, Rakasz EG, Friedrich TC, Wilson NA, Allison DB, Watkins DI. 2008. Patterns of CD8⁺ immunodominance may influence the ability of Mamu-B*08-positive macaques to naturally control simian immunodeficiency virus SIVmac239 replication. *J. Virol.* 82:1723–1738. <http://dx.doi.org/10.1128/JVI.02084-07>.
 35. Valentine LE, Loffredo JT, Bean AT, León EJ, MacNair CE, Beal DR, Piskowski SM, Klimentidis YC, Lank SM, Wiseman RW, Weinfurter JT, May GE, Rakasz EG, Wilson NA, Friedrich TC, O'Connor DH, Allison DB, Watkins DI. 2009. Infection with “escaped” virus variants impairs control of simian immunodeficiency virus SIVmac239 replication in Mamu-B*08-positive macaques. *J. Virol.* 83:11514–11527. <http://dx.doi.org/10.1128/JVI.01298-09>.
 36. Matano T, Kano M, Nakamura H, Takeda A, Nagai Y. 2001. Rapid appearance of secondary immune responses and protection from acute CD4 depletion after a highly pathogenic immunodeficiency virus challenge in macaques vaccinated with a DNA prime/Sendai virus vector boost regimen. *J. Virol.* 75:11891–11896. <http://dx.doi.org/10.1128/JVI.75.23.11891-11896.2001>.
 37. Kawada M, Tsukamoto T, Yamamoto H, Iwamoto N, Kurihara K, Takeda A, Moriya C, Takeuchi H, Akari H, Matano T. 2008. Gag-specific cytotoxic T-lymphocyte-based control of primary simian immunodeficiency virus replication in a vaccine trial. *J. Virol.* 82:10199–10206. <http://dx.doi.org/10.1128/JVI.01103-08>.
 38. Kawada M, Igarashi H, Takeda A, Tsukamoto T, Yamamoto H, Dohki S, Takiguchi M, Matano T. 2006. Involvement of multiple epitope-specific cytotoxic T-lymphocyte responses in vaccine-based control of simian immunodeficiency virus replication in rhesus macaques. *J. Virol.* 80:1949–1958. <http://dx.doi.org/10.1128/JVI.80.4.1949-1958.2006>.
 39. Nomura T, Yamamoto H, Shiino T, Takahashi N, Nakane T, Iwamoto N, Ishii H, Tsukamoto T, Kawada M, Matsuoka S, Takeda A, Terahara K, Tsunetsugu-Yokota Y, Iwata-Yoshikawa N, Hasegawa H, Sata T, Naruse TK, Kimura A, Matano T. 2012. Association of major histocompatibility complex class I haplotypes with disease progression after simian immunodeficiency virus challenge in Burmese rhesus macaques. *J. Virol.* 86:6481–6490. <http://dx.doi.org/10.1128/JVI.07077-11>.
 40. Naruse TK, Chen Z, Yanagida R, Yamashita T, Saito Y, Mori K, Akari H, Yasutomi Y, Miyazawa M, Matano T, Kimura A. 2010. Diversity of MHC class I genes in Burmese-origin rhesus macaques. *Immunogenetics* 62:601–611. <http://dx.doi.org/10.1007/s00251-010-0462-z>.
 41. Argüello JR, Little AM, Pay AL, Gallardo D, Rojas I, Marsh SG, Goldman JM, Madrigal JA. 1998. Mutation detection and typing of polymorphic loci through double-strand conformation analysis. *Nat. Genet.* 18:192–194. <http://dx.doi.org/10.1038/ng0298-192>.
 42. Kawada M, Tsukamoto T, Yamamoto H, Takeda A, Igarashi H, Wat-

- kings DI, Matano T. 2007. Long-term control of simian immunodeficiency virus replication with central memory CD4⁺ T-cell preservation after nonsterile protection by a cytotoxic T lymphocyte-based vaccine. *J. Virol.* 81:5202–5211. <http://dx.doi.org/10.1128/JVI.02881-06>.
43. Yamamoto H, Kawada M, Takeda A, Igarashi H, Matano T. 2007. Postinfection immunodeficiency virus control by neutralizing antibodies. *PLoS One* 2:e540. <http://dx.doi.org/10.1371/journal.pone.0000540>.
 44. Kestler HW, III, Ringler DJ, Mori K, Panicali DL, Sehgal PK, Daniel MD, Desrosiers RC. 1991. Importance of the *nef* gene for maintenance of high virus loads and for development of AIDS. *Cell* 65:651–662. [http://dx.doi.org/10.1016/0092-8674\(91\)90097-1](http://dx.doi.org/10.1016/0092-8674(91)90097-1).
 45. Shibata R, Maldarelli F, Siemon C, Matano T, Parta M, Miller G, Fredrickson T, Martin MA. 1997. Infection and pathogenicity of chimeric simian-human immunodeficiency viruses in macaques: determinants of high virus loads and CD4 cell killing. *J. Infect. Dis.* 176:362–373. <http://dx.doi.org/10.1086/514053>.
 46. Takeda A, Igarashi H, Nakamura H, Kano M, Iida A, Hirata T, Hasegawa M, Nagai Y, Matano T. 2003. Protective efficacy of an AIDS vaccine, a single DNA priming followed by a single booster with a recombinant replication-defective Sendai virus vector, in a macaque AIDS model. *J. Virol.* 77:9710–9715. <http://dx.doi.org/10.1128/JVI.77.17.9710-9715.2003>.
 47. Schindler M, Münch J, Brenner M, Stahl-Hennig C, Skowronski J, Kirchhoff F. 2004. Comprehensive analysis of *nef* functions selected in simian immunodeficiency virus-infected macaques. *J. Virol.* 78:10588–10597. <http://dx.doi.org/10.1128/JVI.78.19.10588-10597.2004>.
 48. Donahoe SM, Moretto WJ, Samuel RV, Metzner KJ, Marx PA, Hanke T, Connor RI, Nixon DF. 2000. Direct measurement of CD8⁺ T cell responses in macaques infected with simian immunodeficiency virus. *Virology* 272:347–356. <http://dx.doi.org/10.1006/viro.2000.0404>.
 49. Iwamoto N, Tsukamoto T, Kawada M, Takeda A, Yamamoto H, Takeuchi H, Matano T. 2010. Broadening of CD8⁺ cell responses in vaccine-based simian immunodeficiency virus controllers. *AIDS* 24:2777–2787. <http://dx.doi.org/10.1097/QAD.0b013e3283402206>.
 50. Nakamura M, Takahara Y, Ishii H, Sakawaki H, Horiike M, Miura T, Igarashi T, Naruse TK, Kimura A, Matano T, Matsuoka S. 2011. Major histocompatibility complex class I-restricted cytotoxic T lymphocyte responses during primary simian immunodeficiency virus infection in Burmese rhesus macaques. *Microbiol. Immunol.* 55:768–773. <http://dx.doi.org/10.1111/j.1348-0421.2011.00384.x>.
 51. Frahm N, Kiepiela P, Adams S, Linde CH, Hewitt HS, Sango K, Feeny ME, Addo MM, Lichterfeld M, Lahaie MP, Pae E, Wurcel AG, Roach T, St. John MA, Altfeld M, Marincola FM, Moore C, Mallal S, Carrington M, Heckerman D, Allen TM, Mullins JI, Korber BT, Goulder PJ, Walker BD, Brander C. 2006. Control of human immunodeficiency virus replication by cytotoxic T lymphocytes targeting subdominant epitopes. *Nat. Immunol.* 7:173–178. <http://dx.doi.org/10.1038/ni1281>.
 52. Friedrich TC, Valentine LE, Yant LJ, Rakasz EG, Piaskowski SM, Furlott JR, Weisgrau KL, Burwitz B, May GE, León EJ, Soma T, Napoe G, Capuano SV, III, Wilson NA, Watkins DI. 2007. Subdominant CD8⁺ T-cell responses are involved in durable control of AIDS virus replication. *J. Virol.* 81:3465–3476. <http://dx.doi.org/10.1128/JVI.02392-06>.
 53. Brennan CA, Ibarondo FJ, Sugar CA, Hausner MA, Shih R, Ng HL, Detels R, Margolick JB, Rinaldo CR, Phair J, Jacobson LP, Yang OO, Jamieson BD. 2012. Early HLA-B*57-restricted CD8⁺ T lymphocyte responses predict HIV-1 disease progression. *J. Virol.* 86:10505–10516. <http://dx.doi.org/10.1128/JVI.00102-12>.



Development of the 8-aza-3-bromo-7-hydroxycoumarin-4-ylmethyl group as a new entry of photolabile protecting groups



Hikaru Takano^a, Tetsuo Narumi^{a,*}, Nami Ohashi^a, Akinobu Suzuki^b, Toshiaki Furuta^b, Wataru Nomura^a, Hirokazu Tamamura^{a,*}

^a *Institution of Biomaterial and Bioengineering, Tokyo Medical and Dental University, 2-3-10 Kandasurugadai, Chiyoda-ku, Tokyo 101-0062, Japan*

^b *Department of Biomolecular Science, Toho University, 2-2-1 Miyama, Funabashi, Chiba 274-8510, Japan*

ARTICLE INFO

Article history:

Received 5 March 2014

Received in revised form 22 April 2014

Accepted 22 April 2014

Available online 30 April 2014

Keywords:

Azacoumarin

Photolabile protecting groups

Caged compounds

Photolytic efficiency

Hydrophilicity

ABSTRACT

A significant substitution effect of the position of the bromo group on the photosensitivity of the 8-azacoumarin chromophore leads to the development of a highly photosensitive 8-aza-3-bromo-7-hydroxycoumarin-4-ylmethyl (aza-3-Bhc) group that shows excellent photolytic efficiency and hydrophilicity with long-wavelength absorption maxima. The newly identified aza-3-Bhc group can be applied to caged glutamates for ester-type and carbamate-type protections of carboxyl and amino functionalities.

© 2014 Elsevier Ltd. All rights reserved.

1. Introduction

Photosensitive biologically active compounds (referred to as caged compounds) have attracted considerable attention due to their practical potentials as phototriggers of biological functions.¹ Progress in the field has been driven by the development of new photolabile protecting group types,² such as nitrobenzyl,³ benzoin,⁴ phenacyl,⁵ and coumarin.⁶ Although a number of chromophores have been applied to photolabile protecting groups, 8-azacoumarin derivatives have not been applied to the caged compounds until our identification of several advantages as an attractive chromophore for caging chemistry, such as excellent water solubility, high molar absorptivity, and efficient photorelease at low pH as described in our previous report.⁷ This report describes the unexpected substitution effects on the photosensitivity of 8-azacoumarin chromophore, leading to the development of a novel 8-aza-3-bromo-7-hydroxycoumarin-4-ylmethyl caging group (aza-3-Bhc **1**) that shows excellent photolytic efficiency and hydrophilicity with long-wavelength absorption maxima and high molar absorptivity,

whose features are superior to those of the 6-bromo derivatives **2** (Fig. 1).

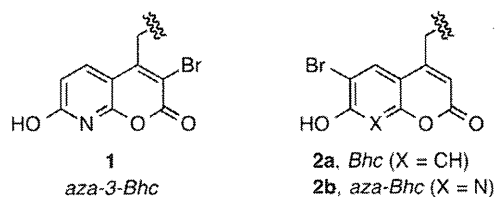


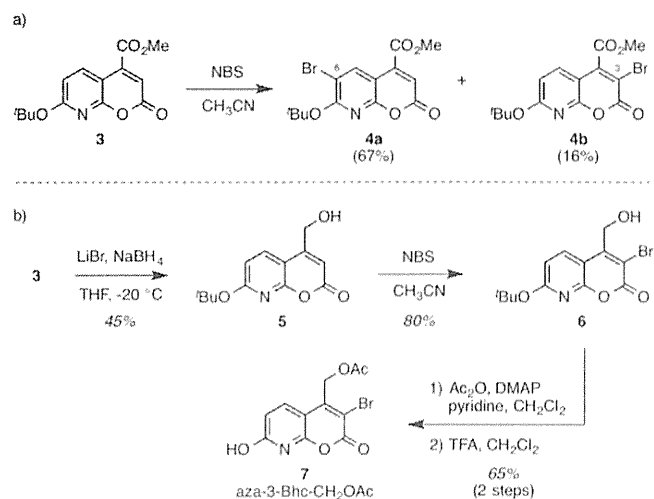
Fig. 1. Structures of azacoumarin- and coumarin-based Bhc groups.

2. Results and discussion

Our study on the development of the aza-3-Bhc group emerged from the bromination of azacoumarin derivative **3** that provided the 6-brominated compound **4a** in a 67% yield as a major product,⁷ accompanied with a 16% yield of the 3-brominated compound **4b** as a minor product (Scheme 1a, Supplementary data). Bromination of the coumarin chromophore provides several advantages for photolysis reactions including lowering the pK_a of the adjacent hydroxyl group accelerating the formation of the strongly absorbing anion and the promotion of intersystem crossing to the triplet, which is considered to be the photochemically reactive state.^{6d}

* Corresponding authors. Tel./fax: +81 53 478 1198 (T.N.); tel.: +81 3 5280 8036; fax: +81 3 5280 8039 (H.T.); e-mail addresses: tnarumi@ipc.shizuoka.ac.jp (T. Narumi), tamamura.mr@tmd.ac.jp (H. Tamamura).

[†] Present address. Department of Applied Chemistry and Biochemical Engineering, Faculty of Engineering, Shizuoka University, Hamamatsu, Shizuoka 432-8561, Japan.



Scheme 1. Synthesis of brominated 8-azacoumarin esters **4** and aza-3-Bhc-CH₂OAc **7**.

Preliminary studies revealed that the 8-aza-7-hydroxycoumarin chromophore as well as the 6-bromo-7-hydroxycoumarin has a pK_a value, which is lower than 7.4, and mostly assumes the deprotonated (ionic) form under physiological conditions without additional electron-withdrawing groups. Therefore, the absorption spectrum of **9** has a single peak as the spectrum of **8** (Fig. 2). These features imply the possibility that the regioisomeric 3-brominated 8-azacoumarin chromophore would also work as a hydrophilic caging group. Furthermore, several papers⁸ that identified strong substitution effects on quinolone chromophores prompted us to invoke that the substitution pattern could positively affect photophysical and photochemical properties of 8-azacoumarin chromophore.

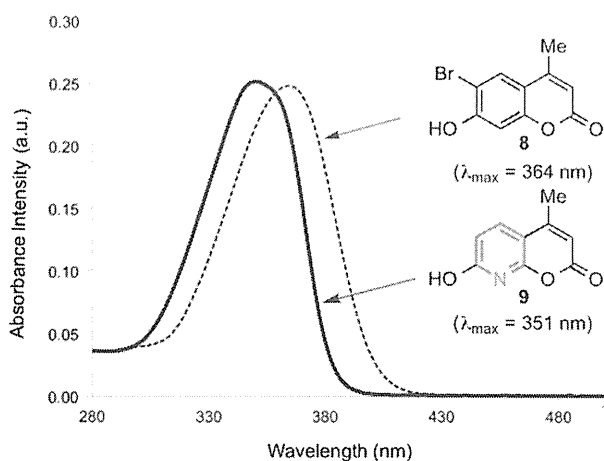


Fig. 2. Absorption spectra of Bhc derivative **8** (dash line) and 8-aza-hc **9** (solid line).

The 3-brominated acetate aza-3-Bhc-CH₂OAc **7** was synthesized from **3** in four steps (Scheme 1b). Briefly, reduction of **3** with LiBH₄ gave the corresponding alcohol **5** in moderate yield. In contrast with the bromination of **3** that gave a mixture of regioisomers, the bromination of alcohol **5** proceeded regioselectively to provide the 3-brominated alcohol **6** in 80% yield, which was subjected to acetylation followed by TFA treatment to give the desired aza-3-Bhc-CH₂OAc **7**.

Initially, we investigated the photophysical and hydrophilic behaviors of aza-3-Bhc-CH₂OAc **7** (Table 1). Compared with the

Table 1
Photophysical and hydrophilic properties of aza-3-Bhc-CH₂OAc **7**, aza-Bhc-CH₂OAc **10**, and Bhc-CH₂OAc **11**

Compd	λ_{\max}^a (nm)	ϵ_{\max}^b (M ⁻¹ cm ⁻¹)	C_s^c (μ M)	pK_a^d
Aza-3-Bhc-CH ₂ OAc (7)	378	27,086	3260	5.08
Aza-Bhc-CH ₂ OAc (10)	362	21,107	10,832	4.22
Bhc-CH ₂ OAc (11)	370	16,584	602	5.88

^a Long-wavelength absorption maxima in PBS (0.1% DMSO).

^b Molar absorptivity at the absorption maxima.

^c Concentration at saturation in PBS (0.1% DMSO).

^d Determined using citric/phosphate buffer in the pH range 2.6–7.0.

original Bhc-CH₂OAc **11**, the absorption maximum of **7** shifted to longer wavelength from 370 nm for **11** to 378 nm for **7**, whereas that of **10** shifted to shorter wavelength (λ_{\max} =362 nm). The molar absorptivity at the maximum wavelength (ϵ_{\max}) of **7** is 27,086 M⁻¹ cm⁻¹, which is also higher than those of **10** (ϵ_{\max} =21,107 M⁻¹ cm⁻¹) and **11** (ϵ_{\max} =16,584 M⁻¹ cm⁻¹). These results indicated that the 3-brominated 8-azacoumarin would be a superior chromophore to the 6-brominated coumarins. As expected, aza-3-Bhc-CH₂OAc **7** has a pK_a value below the physiological pH and also shows high aqueous solubility, which is important for the photorelease of high concentrations of the caged compounds under physiological conditions. HPLC monitoring of the hydrolysis stability revealed that while aza-3-Bhc-CH₂OAc **7** was more sensitive to hydrolysis in PBS (pH 7.4) than aza-Bhc-CH₂OAc **10**, the hydrolysis stability of **7** in KMOPS buffer (10 mM MOPS; 3-morpholinopropane-1-sulfonic acid, and 100 mM KCl, pH 7.1) is comparable to that of **10** (Fig. 3).

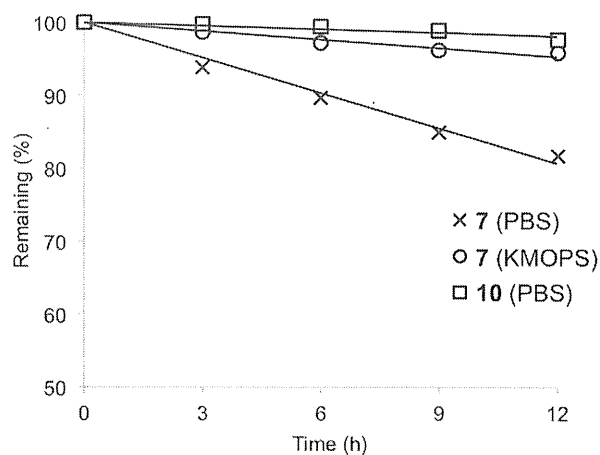
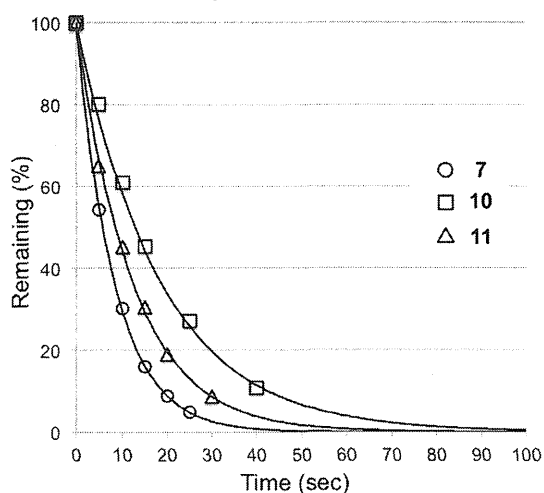


Fig. 3. Hydrolysis stability of compounds **7** and **10** at room temperature in dark. Time course of compounds **7** and **10** in PBS or KMOPS was analyzed by reversed-phase HPLC.

Having recognized promising photophysical and hydrophilic behaviors of the 3-brominated 8-azacoumarin chromophore, we evaluated the photochemical properties of aza-3-Bhc-CH₂OAc **7** under the photolysis in 5 μ M KMOPS buffer solution at pH 7.2 at 350 nm. The time course of photolysis reaction of **7** was monitored by HPLC in terms of the consumption of the starting materials (Table 2), and indicates that the photolytic reaction at 350 nm of **7** follows a single-exponential decay as in the result of the original Bhc compound **11**. The time to reach 90% conversion (t_{90}) for photolysis of **7** is 19 s, which is shorter than those of the 6-

Table 2
Time course for photolysis reactions of aza-3-Bhc-CH₂OAc **7**, aza-Bhc-CH₂OAc **10**, and Bhc-CH₂OAc **11** and selected photochemical properties



Compd	t_{90} (s)	ϵ_{350}^a (M ⁻¹ cm ⁻¹)	Φ_{chem}^b	$\epsilon_{350} \cdot \Phi_{chem}^c$
Aza-3-Bhc-CH ₂ OAc (7)	19	20,175	0.17	2667
Aza-Bhc-CH ₂ OAc (10)	42	20,583	0.059	1211
Bhc-CH ₂ OAc (11)	28	13,774	0.13	1806

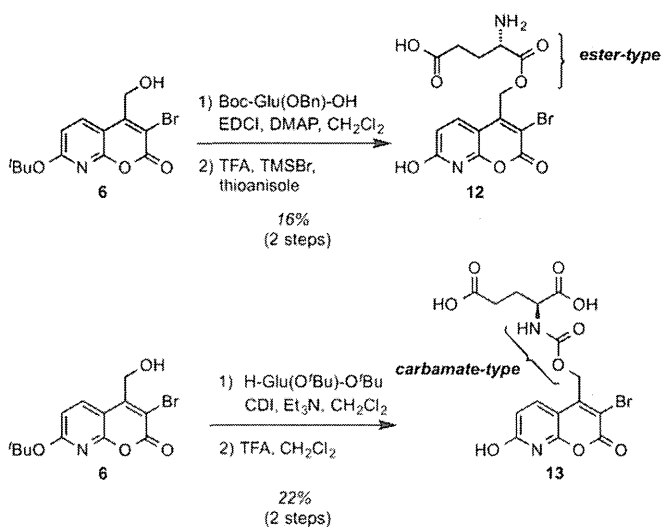
^a Molar absorptivity at 350 nm.

^b Quantum yields for the disappearance of starting materials upon irradiation at 350 nm.

^c Product of the photolysis quantum yield and molar absorptivity.

brominated coumarins **10** and **11** (t_{90} =42 s for **10** and 28 s for **11**, respectively). The photolysis quantum yields of disappearance of starting materials were calculated from the single decay curves using the equation $\Phi = 1/(I \times 10^3 \epsilon t_{90})$ as reported by Tsien.⁹ Notably, the quantum yield of disappearance of **7** (Φ_{chem} =0.17) is approximately three times higher than that of **10** (Φ_{chem} =0.059) and significantly higher than that of **11** (Φ_{chem} =0.13). In addition, the photolytic efficiency,¹⁰ the product of the photolysis quantum yield (Φ_{chem}) and molar absorptivity (ϵ) of **7** ($\epsilon_{350} \cdot \Phi_{chem}$ =2667), is approximately 1.5–2.2-fold higher than that of **10** ($\epsilon_{350} \cdot \Phi_{chem}$ =1211) and **11** ($\epsilon_{350} \cdot \Phi_{chem}$ =1806). These results indicate that the bromo substitution on position 3 of the 8-azacoumarin chromophore leads not only to improve the photophysical behavior but also to increase the photosensitivity. Although the reason for the significant enhancement of photochemical reactivity of **7** is not fully understood at this stage, these observations suggest that the aza-3-Bhc group has a powerful set of photophysical, photochemical, and hydrophilic properties for caging chemistry.

Next, we examined the synthetic methods for the introduction of the aza-3-Bhc group to biologically relevant compounds (Scheme 2). The aza-3-Bhc group is not limited to the caging group for ester-types. In addition to the α -Glu ester **12**, the aza-3-Bhc group can be applied to the α -Glu carbamate **13** for the protection of an amino functionality, which can be removed efficiently with light of wavelength of 365 nm to produce the corresponding alcohol.¹¹ Compared to the corresponding Bhc-protected compounds **14** and **15**,^{6d} both aza-3-Bhc-protected compounds **12** and **13** showed improved photosensitivity (Table 3). The time to reach 90% conversion (t_{90}) for photolysis of **12** is 32 s, which corresponds to be approximately 20% faster than that of the corresponding Bhc-protected α -Glu ester **14** (t_{90} of **14**=38 s). A similar superiority of the aza-3-Bhc group was observed with the carbamate substrates **13** and **15**. In accordance with the greater quantum yields of disappearance and comparable molar absorptivities, the photolytic efficiency of both **12** and **13** is higher than those of **14** and **15** (relative



Scheme 2. Synthesis of aza-3-Bhc-caged glutamates.

value of $\epsilon \cdot \Phi$ of **12/14**=1.19 and of **13/15**=1.27). These results indicate that the newly identified aza-3-Bhc chromophore can serve as a variant of Bhc chromophore in biologically relevant compounds. Further studies for the application of the 8-aza-3-Bhc group to the protection of other functionalities, such as alcohols, phosphoric acids, and thiols are in progress.

3. Conclusion

We have reported the development of the aza-3-Bhc group as a new entry of photolabile protecting groups for caging chemistry through the strong influence of the position of a bromo substituent on the photosensitivity of the 8-azacoumarin chromophore. The 3-brominated 8-azacoumarin **7** is considerably more efficient than the 6-brominated regioisomer **10**. Aza-3-Bhc-CH₂OAc **7** shows excellent photolytic efficiency with a bathochromic shift of the absorption maximum of 8-azacoumarin from 362 to 378 nm. Moreover, we have disclosed the potentials of the aza-3-Bhc group as protecting groups of carboxyl and amino functionalities for caged glutamates. A key to the development of the aza-3-Bhc group is the acidic azacoumarin chromophore, whose feature can provide a new opportunity to improve the photosensitivity by chemical modifications that are distinct from those in previous approaches. Efforts to elucidate the reason for the markedly enhanced photosensitivity by the 3-bromo substituent and studies on the two-photon sensitivity of the 8-azacoumarin chromophore are currently in progress.

4. Experimental section

4.1. General methods

All reactions utilizing air- or moisture-sensitive reagents were performed in dried glassware under an atmosphere of nitrogen, using commercially supplied solvents and reagents unless otherwise noted. CH₂Cl₂ was distilled from CaH₂ and stored over molecular sieves. Thin-layer chromatography (TLC) was performed on Merck 60F₂₅₄ precoated silica gel plates and were visualized by fluorescence quenching under UV light and by staining with phosphomolybdic acid, *p*-anisaldehyde, or ninhydrin, respectively. Flash column chromatography was carried out using silica gel 60 N (Kanto Chemical Co., Inc.).

Table 3
Selected photophysical and photochemical properties of aza-3-Bhc-caged glutamates **12** and **13**, and Bhc-caged glutamates **14** and **15**

Compd	λ_{\max}^a (nm)	ϵ_{\max}^b ($M^{-1} \text{ cm}^{-1}$)	ϵ_{365}^c ($M^{-1} \text{ cm}^{-1}$)	t_{90}^d (s)	Φ_{chem}^e	$\epsilon_{365} \cdot \Phi_{\text{chem}}^f$	rel. $\epsilon \cdot \Phi^g$
Aza-3-Bhc-Glu-ester (12)	378	13,648	12,153	32	0.17	2063	1.19
Aza-3-Bhc-Glu-carbamate (13)	376	17,068	15,623	10	0.43	6717	1.27
Bhc-Glu-ester (14)	370	16,912	16,466	38	0.11	1740	—
Bhc-Glu-carbamate (15)	370	17,822	17,636	13	0.30	5280	—

^a Long-wavelength absorption maxima in PBS (0.1% DMSO).^b Molar absorptivity at the absorption maxima.^c Molar absorptivity at 365 nm.^d Time to reach 90% conversion.^e Quantum yields for the disappearance of starting materials upon irradiation at 365 nm.^f Photolytic efficiency: product of the photolysis quantum yield and molar absorptivity.^g Relative value of photolytic efficiency [aza-3-Bhc/Bhc]. For full experimental protocol, see Supplementary data.

4.2. Characterization data

¹H NMR (400 or 500 MHz) and ¹³C NMR (125 MHz) spectra were recorded using a Bruker Avance II spectrometer with a CryoProbe. Chemical shifts are reported in δ (ppm) relative to Me₄Si (in CDCl₃) as internal standard. Infrared (IR) spectra were recorded on a JASCO FT/IR 4100, and are reported as wavenumber (cm⁻¹). Low- and high-resolution mass spectra were recorded on a Bruker Daltonics micrOTOF (ESI-MS) spectrometers in the positive and negative detection modes.

4.3. HPLC condition

For analytical HPLC, a Cosmosil C18-ARII column (4.6×250 mm, Nacalai Tesque, Inc., Kyoto, Japan) was employed with a linear gradient of MeCN containing 0.1% (v/v) TFA at a flow rate of 1 cm³ min⁻¹ an Agilent HP 1100 system with DAD detection (Agilent Technologies JAPAN Ltd., Tokyo, Japan) and JASCO PU-2086 plus (JASCO corporation, Ltd., Tokyo, Japan), and eluting products were detected by UV at 340 nm.

4.4. Experimental procedures of 8-azacoumarin derivatives **5**, **6**, **7**, **12**, and **13**

4.4.1. 7-(tert-Butoxy)-4-(hydroxymethyl)-2H-pyrano[2,3-b]pyridin-2-one (5). A suspension of LiBr (1.09 g, 12.6 mmol) and NaBH₄ (410.2 mg, 10.8 mmol) in THF (36.0 mL) was stirred under nitrogen at 50 °C for 2 h, producing the solution of LiBH₄ (ca. 0.3 M). To the solution was added compound **3** (1.03 g, 3.72 mmol) in THF (36.0 mL), and the mixture was stirred at -20 °C for 2 h. The reaction mixture was quenched by 1 M HCl aq, and the organic layer was removed under reduced pressure. The residue was extracted with EtOAc, washed with brine, and dried over Na₂SO₄. Concentration under reduced pressure followed by flash column chromatography over silica gel with *n*-hexane/EtOAc (1:1) gave the title compound **5** (411.8 mg, 45% yield) as white powder. Mp: 236–244 °C (dec); ¹H NMR (500 MHz, CDCl₃) δ 1.64 (s, 9H), 4.85 (m, 2H), 6.45 (m, 1H), 6.60 (m, 1H), 7.74 (m, 1H); ¹³C NMR (125 MHz, CDCl₃) δ 28.3, 60.9, 82.5, 104.9, 109.1, 110.5, 134.6, 153.9, 157.4, 161.5, 164.6; IR (ATR) ν 3395 (OH), 1704 (CO); HRMS (ESI), *m/z* calcd for C₉H₈NO₄ [M-*tert*-Bu+2H]⁺ 194.0453, found 194.0450.

4.4.2. 3-Bromo-7-(tert-butoxy)-4-(hydroxymethyl)-2H-pyrano[2,3-b]pyridin-2-one (6). To a solution of compound **5** (121.4 mg, 0.487 mmol) in CH₃CN (1.37 mL) was added NBS (428.6 mg, 125 mmol), and the mixture was stirred at room temperature for 4 h. After being concentrated under reduced pressure, the residue was dissolved in EtOAc, washed with H₂O, and dried over Na₂SO₄. Concentration under reduced pressure followed by flash column chromatography over silica gel with *n*-hexane/EtOAc (1:1) gave the title compound **6** (127.1 mg, 80% yield) as a dark green solid. Mp:

254–257 °C (dec); ¹H NMR (500 MHz, CDCl₃) δ 1.64 (s, 9H), 5.02 (s, 2H), 6.67 (m, 1H), 8.13 (m, 1H); ¹³C NMR (125 MHz, CDCl₃) δ 28.7, 61.9, 82.9, 106.1, 109.3, 111.3, 136.8, 150.3, 156.23, 157.7, 164.7; IR (ATR) ν 3465 (OH) 2977 (CH), 2929 (CH), 1707 (CO), HRMS (ESI), *m/z* calcd for C₁₃H₁₄BrNNaO₄ [M+Na]⁺ 350.0004, found 350.0000.

4.4.3. (3-Bromo-7-hydroxy-2-oxo-2H-pyrano[2,3-b]pyridin-4-yl)methylacetate (7). To a solution of compound **6** (127.1 mg, 0.389 mmol) and DMAP (6.20 mg, 0.0507 mmol) in CH₂Cl₂ (5.6 mL) were added sequentially pyridine (313.1 μ L, 3.89 mmol) and acetic anhydride (183.7 μ L, 1.94 mmol), and the mixture was stirred at room temperature for 1 h. The reaction mixture was diluted with CH₂Cl₂, washed with NaHCO₃ aq, and dried over Na₂SO₄. Concentration under reduced pressure gave the corresponding acetate (138.1 mg, 96% yield). To a solution of the corresponding acetate (138.1 mg, 0.374 mmol) in CH₂Cl₂ (1 mL) was added trifluoroacetic acid (1 mL), and the mixture was stirred at room temperature for 30 min. Concentration under reduced pressure followed by flash column chromatography over silica gel with CHCl₃/MeOH (5:1) to give the title compound **7** (80.1 mg, 68% yield) as a white solid. Mp: 273–276 °C (dec); ¹H NMR (500 MHz, CD₃OD) δ 1.99 (s, 3H), 5.35 (s, 2H), 6.53 (d, *J*=9.0 Hz, 1H), 7.97 (d, *J*=9.0 Hz, 1H); ¹³C NMR (125 MHz, CD₃OD) δ 20.5, 61.1, 102.0, 106.1, 109.4, 136.2, 150.9, 158.4, 160.4, 166.8, 170.0; IR (ATR) ν 2923 (OH) 1736 (CO), HRMS (ESI), *m/z* calcd for C₁₁H₈BrNNaO₅ [M+Na]⁺ 335.9484, found 335.9485.

4.4.4. (S)-4-Amino-5-((3-bromo-7-hydroxy-2-oxo-2H-pyrano[2,3-b]pyridin-4-yl)methoxy)-5-oxopentanoic acid (12). To a solution of Boc-Glu(OBn)-OH (158.0 mg, 0.468 mmol), EDCI·HCl (541.2 mg, 2.82 mmol), and DMAP (13.8 mg, 0.113 mmol) in CH₂Cl₂ (10.2 mL) was added compound **6** (100.7 mg, 0.308 mmol), and the mixture was stirred at room temperature for 24 h. The mixture was poured into water and extracted with EtOAc, and dried over Na₂SO₄. Concentration under reduced pressure gave the crude compound (321.9 mg), which was used in the next step without further purification. A solution of the crude compound (321.9 mg, 0.498 mmol), 1 M TMS-Br/TFA (3.32 mL), and 1 M thioanisole/TFA (3.32 mL) was stirred at room temperature for 3 h. Purification by preparative HPLC (Gradient: 0 min, 0% CH₃CN in H₂O; 90 min, 40% CH₃CN in H₂O) followed by lyophilization to give a title compound **12** (23.7 mg, 16% yield) as a pale purple solid. Mp: 149–154 °C (dec); ¹H NMR (500 MHz, CD₃OD) δ 2.06 (m, 2H), 2.39 (m, 2H), 4.10 (m, 1H), 5.56 (m, 2H), 6.60 (d, *J*=8.5 Hz, 1H), 8.06 (d, *J*=8.5 Hz, 1H); ¹³C NMR (125 MHz, CD₃OD) δ 26.6, 30.2, 53.2, 64.7, 106.3, 110.4, 112.0, 139.1, 147.5, 157.9, 158.3, 166.6, 169.9, 175.4; IR (ATR) ν 3505 (NH), 2981 (OH), 2865 (CH), 1737 (CO), 1690 (CO) 1682 (CO), HRMS (ESI), *m/z* calcd for C₁₄H₁₄BrN₂O₇ [M+H]⁺ 400.9984, found 400.9981.

4.4.5. (S)-2-(((3-bromo-7-hydroxy-2-oxo-2H-pyrano[2,3-b]pyridin-4-yl)methoxy)carbonyl)amino)-pentanedioic acid (13). To a solution

of CDI (25.4 mg, 0.157 mmol) of CH_2Cl_2 was added **6** (48.5 mg, 0.148 mmol), and the mixture stirred at 0 °C for 1 h. After H-Glu(O^tBu)-O^tBu (90.4 mg, 0.306 mmol) and Et₃N (52.3 μL , 0.375 mmol) were added, the mixture was stirred at room temperature for additional 12 h. The reaction mixture was concentrated with reduced pressure. The residue was diluted with Et₂O, and washed with water and brine, dried over Na₂SO₄. Concentration under reduced pressure gave the crude compound (168.1 mg), which was used in the next step without further purification. To a solution of the crude compound (168.1 mg, 0.275 mmol) in CH_2Cl_2 (0.90 mL) was added TFA (2.7 mL), and the mixture was stirred at room temperature for 1 h. Purification by preparative HPLC (Gradient: 0 min, 5% CH_3CN in H_2O ; 90 min, 40% CH_3CN in H_2O) followed by lyophilization to give a title compound **13** (17.6 mg, 22% yield) as a pale green solid. Mp: 196–198 °C (dec); ¹H NMR (500 MHz, CD₃OD) δ 1.88 (m, 1H), 2.16 (m, 1H), 2.38 (m, 2H), 4.19 (m, 1H), 5.46 (s, 2H), 6.68 (m, 1H), 8.19 (m, 1H); ¹³C NMR (125 MHz, CD₃OD) δ 27.8, 31.1, 54.8, 64.0, 106.3, 110.4, 110.8, 139.6, 149.4, 157.6 (2C), 158.4, 166.3, 175.2, 176.3; IR (ATR) ν 3306 (NH), 2981 (OH), 1742 (CO), 1698 (CO), HRMS (ESI), m/z calcd for C₁₅H₁₃BrN₂NaO₉ [M+Na]⁺ 466.9702, found 466.9701.

4.5. Determination of saturated concentrations

Saturated concentrations of compounds were calculated from the standard curves that related peak area (340 nm) against known concentration of compounds in PBS.

4.6. Determination of the pK_a values

The pK_a values of compounds were estimated from the titration curves of absorbance against pH using 10 μM substrate solution in citric/phosphate buffer solution in the pH range 2.6–7.0 by adjusting the acidity with 10 μL of 2 M NaOH sequentially. The pH values were analyzed by a sensitive pH meter (HORIBA, F51).

4.7. Photolysis and quantum efficiency measurement

Into a Pyrex test tube of 12 mm diameter was placed 2 mL of 10 μM substrate solution in KMOP solution (pH 7.2) containing 0.1% DMSO. The solution was irradiated at 350 nm using four RPR 350 nm lamps (10 mJ s⁻¹). Aliquots of 10 μM were removed periodically and analyzed by HPLC. The light output for the quantum efficiencies measurement was performed using ferrioxalate actinometry.

Acknowledgements

This research was supported by the Naito Foundation, KEN10000322 (Natural Science Scholarship) and in part by a Grant-in-Aid for Young Scientist (B) from the Ministry of Education, Culture, Sports, Science, and Technology.

Supplementary data

This section presents the experimental details, and ¹H and ¹³C NMR spectra. Supplementary data related to this article can be found at <http://dx.doi.org/10.1016/j.tet.2014.04.063>.

References and notes

- (a) *Caged Compounds*; Marriot, G., Ed. *Methods in Enzymology*; Academic: New York, NY, 1998; Vol. 291; (b) Mayer, G.; Heckel, A. *Angew. Chem., Int. Ed.* **2006**, *45*, 4900–4921; (c) Ellis-Davies, G. C. R. *Nat. Methods* **2007**, *4*, 619–628; (d) Lee, H. M.; Larson, D. R.; Lawrence, D. S. *ACS Chem. Biol.* **2009**, *4*, 409–427.
- (a) Briekie, C.; Rohrbach, F.; Gottschalk, A.; Mayer, G.; Heckel, A. *Angew. Chem., Int. Ed.* **2012**, *51*, 8446–8476; (b) Klán, P.; Solomek, T.; Bochet, C. G.; Blanc, A.; Givens, R.; Rubina, M.; Popik, V.; Kostikov, A.; Würz, J. *Chem. Rev.* **2013**, *113*, 119–191.
- Nitrobenzyl-type**: (a) Engels, J.; Schlaeger, E.-J. *J. Med. Chem.* **1977**, *20*, 907–911; (b) Kaplan, J. H.; Forbush, B., III; Hoffman, J. F. *Biochemistry* **1978**, *17*, 1929–1935.
- Benzoin-type**: (a) Sheehan, J. C.; Wilson, R. M. *J. Am. Chem. Soc.* **1964**, *86*, 5277–5281; (b) Givens, R. S.; Athey, P. S.; Kueper, L. W., III; Matuszewski, B.; Xue, J. *J. Am. Chem. Soc.* **1992**, *114*, 8708–8710; (c) Hansen, K. C.; Rock, R. S.; Larsen, R. W.; Chan, S. I. *J. Am. Chem. Soc.* **2000**, *122*, 11567–11568.
- Phenacyl-type**: (a) Sheehan, J. C.; Umezawa, K. *J. Org. Chem.* **1973**, *38*, 3771–3774; (b) Givens, R. S.; Weber, J. F. W.; Jung, A. H.; Park, C.-H. *Methods Enzymol.* **1998**, *291*, 1–29; (c) Conrad, P. G., II; Givens, R. S.; Weber, J. F. W.; Kandler, K. *Org. Lett.* **2000**, *2*, 1545–1547.
- Coumarin-type**: (a) Givens, R. S.; Matuszewski, B. *J. Am. Chem. Soc.* **1984**, *106*, 6860–6861; (b) Furuta, T.; Torigai, H.; Sugimoto, M.; Iwamura, M. *J. Org. Chem.* **1995**, *60*, 3953–3956; (c) Furuta, T.; Iwamura, M. *Methods Enzymol.* **1998**, *291*, 50–63; (d) Furuta, T.; Wang, S. S. H.; Dantzker, J. L.; Dore, T. M.; Bybee, W. J.; Callaway, E. M.; Denk, W.; Tsien, R. Y. *Proc. Natl. Acad. Sci. U.S.A.* **1999**, *96*, 1193–1200; (e) Hagen, V.; Bendig, J.; Fring, S.; Eckardt, T.; Helm, S.; Reuter, D.; Kaupp, U. B. *Angew. Chem., Int. Ed.* **2001**, *40*, 1045–1048; (f) Eckardt, T.; Hagen, V.; Schade, B.; Schmidt, R.; Schweitzer, C.; Bendig, J. *J. Org. Chem.* **2002**, *67*, 703–710; (g) Geisler, D.; Kresse, W.; Wiesner, B.; Bendig, J.; Kettenmann, H.; Hagen, V. *ChemBioChem* **2003**, *4*, 162–170; (h) Nomura, W.; Narumi, T.; Ohashi, N.; Serizawa, Y.; Lewin, N. E.; Blumberg, P. M.; Furuta, T.; Tamamura, H. *ChemBioChem* **2011**, *12*, 535–539.
- Narumi, T.; Takano, H.; Ohashi, N.; Suzuki, A.; Furuta, T.; Tamamura, H. *Org. Lett.* **2014**, *16*, 1184–1187.
- (a) Petit, M.; Tran, C.; Roger, T.; Gallavardin, T.; Dhiman, H.; Palma-Cerda, F.; Blanchard-Desce, M.; Acher, F. C.; Ogden, D.; Dalko, P. I. *Org. Lett.* **2012**, *14*, 6366–6369; (b) Zhu, Y.; Pavlos, C. M.; Toscano, J. P.; Dore, T. M. *J. Am. Chem. Soc.* **2005**, *128*, 4267–4276; (c) Davis, M. J.; Kragor, C. H.; Reddie, K. G.; Wilson, H. C.; Zhu, Y.; Dore, T. M. *J. Org. Chem.* **2009**, *74*, 1721–1729; (d) Laras, Y.; Hugues, V.; Chandrasekaran, Y.; Blanchard-Desce, M.; Acher, F. C.; Pietrancosta, N. *J. Org. Chem.* **2012**, *77*, 8294–8302.
- Tsien, R. Y.; Zuker, R. S. *Biophys. J.* **1986**, *50*, 843–853.
- Brown, E. B.; Shear, J. B.; Adams, S. R.; Tsien, R. Y.; Webb, W. W. *Biophys. J.* **1999**, *76*, 489–499.
- See Supplementary data for details.

Isostere-Based Design of 8-Azacoumarin-Type Photolabile Protecting Groups: A Hydrophilicity-Increasing Strategy for Coumarin-4-ylmethyls

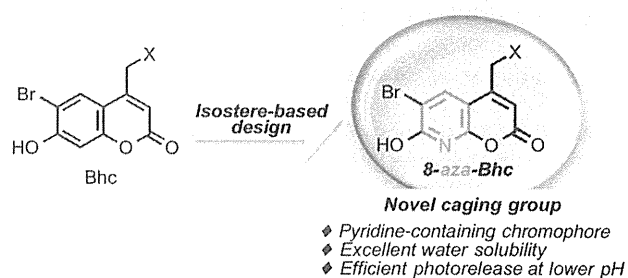
Tetsuo Narumi,^{†,§,¶} Hikaru Takano,^{†,¶} Nami Ohashi,[†] Akinobu Suzuki,[‡] Toshiaki Furuta,[‡] and Hirokazu Tamamura^{*,†}

[†]Institute of Biomaterials and Bioengineering, Tokyo Medical and Dental University, Chiyoda-ku, Tokyo 101-0062, Japan

[‡]Department of Biomolecular Science, Toho University, 2-2-1 Miyama, Funabashi, Chiba 274-8510, Japan

Supporting Information

ABSTRACT: Described is the development of 8-azacoumarin-4-ylmethyl groups as aqueous photolabile protecting groups. A key feature of the strategy is the isosteric replacement of the C7–C8 enol double bond of the Bhc derivative with an amide bond, resulting in conversion of the chromophore from coumarin to 8-azacoumarin. This strategy makes dramatically enhanced water solubility and facile photocleavage possible.



Chemical processes mediated by photolabile protecting groups find numerous utilities in synthetic organic chemistry,¹ chemical biology, and cell biology.² The exceptional utilities of photolabile protecting groups include their mild conditions associated with the photocleavage that can proceed smoothly and quickly even in aqueous conditions and their potential as photoactivatable molecules or caged compounds that enable spatial and temporal control of their biological functions.³ Among various caging groups,^{4–7} coumarins have had widespread applications to caging chemistry in recent years. In particular, the potential of two-photon photolysis with practically useful absorption cross sections (720–900 nm) is among the outstanding advantages of coumarin types such as the 6-bromo-7-hydroxycoumarin-4-ylmethyl (Bhc) group.^{7d} However, one of the drawbacks of coumarin types is their low aqueous solubility. Aqueous solubility is critical for the utility of caged compounds, since hydrophobic caged compounds will be aggregated in physiological conditions and the photocleavage would be plagued by sluggish reactivity.^{7h}

There are a few methods for increasing the aqueous solubility of coumarin chromophores. One successful example is the introduction of one or more hydrophilic carboxyl groups such as BCMACM,⁸ BBHCM,⁹ and DEAC450.¹⁰ Although these approaches effectively achieve the increase of hydrophilicity of coumarin chromophores, the development of new strategies for increasing the hydrophilicity with high photosensitivity remains challenging.

In this report, we disclose a simple and powerful strategy based on the concept of the amide-alkene isosterism for increasing the hydrophilicity of coumarin-type photolabile protecting groups (Figure 1), leading to the development of novel 8-azacoumarin-type protecting groups. The newly

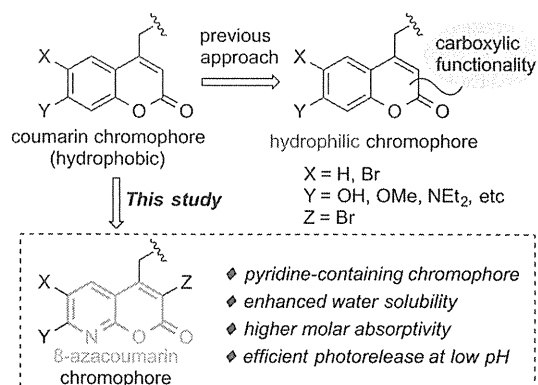


Figure 1. Strategies to increase the hydrophilicity of the coumarin chromophore.

designed 8-azacoumarin-type protecting groups have approximately 10- to 18-fold enhanced solubility in aqueous buffer compared to that of the parent Bhc group and possess photophysical and photochemical properties favorable for caging chemistry. Our presented strategy has the potential to provide new solutions for the development of caged compounds with enhanced hydrophilicity.

Our studies started from the design of novel chromophores with enhanced hydrophilicity (Figure 2). Our approach to increasing hydrophilicity is based on the introduction of polar and hydrophilic amide functionality into the coumarin chromophore. As shown in Figure 2, the C7–C8 enol double

Received: January 7, 2014

Published: February 4, 2014

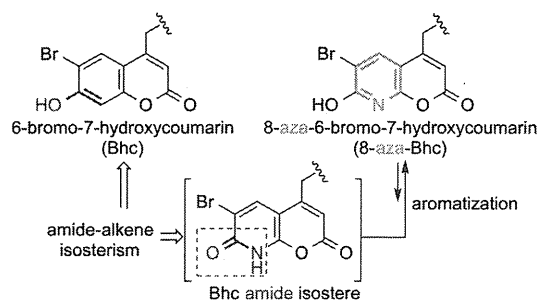


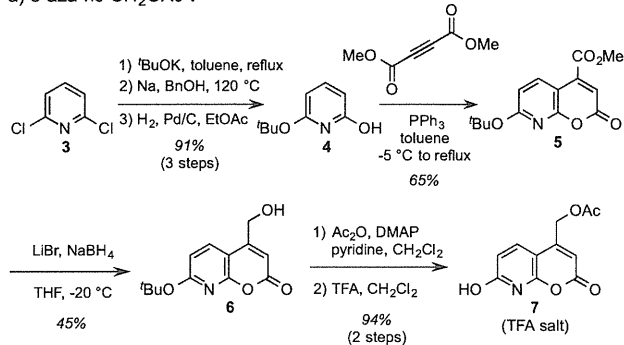
Figure 2. Isostere-based design of an 8-azacoumarin-type photolabile protecting group.

bond of the coumarin chromophore was replaced with an amide bond followed by aromatization of the lactam moiety to form a hydroxypyridine-containing 8-azacoumarin chromophore. This strategy relies on the concept of structural isosterism of amides and alkenes (enols), familiar in medicinal chemistry¹¹ and exemplified by alkene-type dipeptide isosteres,¹² which are regarded as ideal ground state mimetics of dipeptides and thus have been applied to many biologically active peptides.¹³

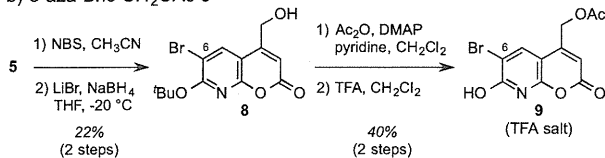
Our synthesis of 8-azacoumarins with a hydroxymethyl group at the C4 position began with 2,6-dichloropyridine 3 (Scheme 1). Successive treatments of 3 with potassium *tert*-

Scheme 1. Synthesis of Azacoumarin Derivatives 7 and 9

a) 8-aza-hc-CH₂OAc 7



b) 8-aza-Bhc-CH₂OAc 9



butoxide and sodium benzyl alkoxide followed by hydrogenolysis of the benzyl group afforded the hydroxypyridine derivative 4 in an excellent yield (91% in 3 steps). Reaction of 4 with dimethyl acetylenedicarboxylate (DMAD) in the presence of PPh₃ provided the desired 8-azacoumarin 5 with an ester functionality at the C4 position in 65% yield.¹⁴ Chemoselective reduction was required for the conversion of this conjugated ester of 5 to the corresponding alcohol, since the lactone moiety of 8-azacoumarin is subject to cleavage by reducing agents. Screening of various reducing agents revealed that the use of LiBH₄ prepared *in situ* in THF at -20 °C afforded acceptable conversion giving the desired 8-azacoumarin

derivative 6 with a hydroxymethyl group at the C4 position, in 45% isolated yield. Compound 6 was subjected to acetylation of the alcohol followed by TFA treatment to give the desired 4-acetoxymethyl-8-aza-hc (8-aza-hc-CH₂OAc, 7). Furthermore, in order to study the substituent (heavy atom) effects^{7d} on the 8-azacoumarin chromophore, the 6-brominated derivative (8-aza-Bhc-CH₂OAc, 9) was also synthesized in a similar manner (Scheme 1b).

The key underlying concept of our approach is the introduction of an amide functionality to the coumarin chromophore to increase the aqueous solubility. The aqueous solubility of 8-azacoumarin derivatives 7 and 9 in PBS (0.1% DMSO) was evaluated with the parent Bhc derivative 10 (Table 1). As expected, 8-azacoumarin derivatives showed

Table 1. Hydrophilic Properties of 8-Azacoumarins 7 and 9 and Bhc Derivative 10

compd	C _s ^a (μM)	pK _a ^b
7	6611	5.67
9	10832	4.22
10	602	5.88 ^c

^aConcentration at saturation in PBS buffer (0.1% DMSO).

^bDetermined using citric/phosphate buffer in the pH range 2.6–7.0.

^cLiterature value = 6.2 in H₂O.¹⁵

hydrophilicity much higher than that of 10; in particular, the saturated concentration (C_s) of 8-aza-Bhc-CH₂OAc 9 was approximately 18-fold greater than that of 10. These results indicate that the replacement of the chromophore involving the conversion of the coumarin into 8-azacoumarin enabled the enhancement of hydrophilicity of the coumarin chromophore. It is noteworthy that 8-aza-Bhc-CH₂OAc 9 showed hydrophilicity higher than that of the nonbrominated compound 7 possibly due to the lower pK_a value (4.22) of the chromophore. In addition, HPLC monitoring of 9 in PBS at room temperature showed that 9 was highly resistant to spontaneous hydrolysis in the dark and that only 2% of 9 was hydrolyzed in 12 h.¹⁶

The photochemical properties of azacoumarin derivatives 7, 9, and 10 in aqueous solutions were examined. 8-Aza-hc-CH₂OAc 7 was subjected to photolysis in 5 μM KMOPS buffer (10 mM MOPS; 4-morpholinepropane-1-sulfonic acid, and 100 mM KCl) solution at pH 7.2 at 350 nm. Figure 3 shows the time courses of photolysis reactions of synthetic compounds in terms of the consumption of the starting materials and indicates that the photolytic reaction of 7 follows a single-exponential decay with the time to reach 50% conversion (*t*₅₀) for photolysis of 7 at 29 s. As expected, introduction of the bromo group resulted in the remarkable increase of the photochemical reactivity; the value of *t*₅₀ for photolysis of 9 is 13 s, which is slightly longer than that of 10 (9 s) but is about 2.3 times shorter than that of 7. Although the photolytic mechanism of 8-azacoumarin derivatives 7 and 9 is not fully understood at this stage, these observations suggest the possibility of 8-azacoumarin-based chromophores working as photolabile protecting groups.

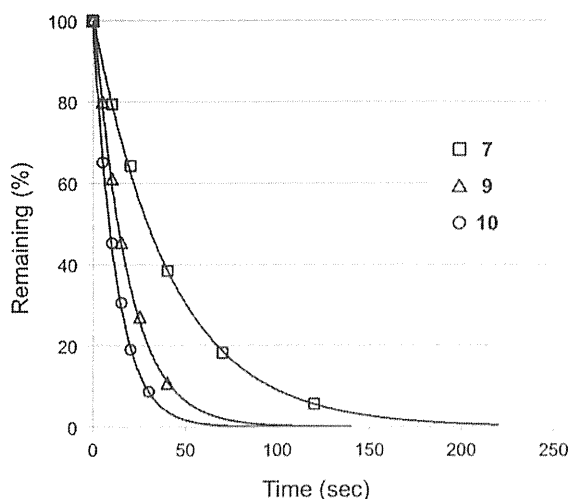


Figure 3. Time courses of photolysis reactions of **7**, **9**, and **10**. Samples were subjected to photolysis in 5 μM KMOPS buffer solution at pH 7.2 at 350 nm (10 mJ/s). All data are the mean values for at least two independent experiments.

Photophysical and photochemical properties of the 8-azacoumarin derivatives **7** and **9** and the Bhc derivative **10** are shown in Table 2. The absorption maxima shifted slightly to

Table 2. Selected Photophysical and Photochemical Properties of Compounds **7**, **9**, and **10**

compd	λ_{max}^a (nm)	ϵ_{max}^b ($\text{M}^{-1}\text{cm}^{-1}$)	ϵ_{350}^c ($\text{M}^{-1}\text{cm}^{-1}$)	Φ_{chem}^d	$\epsilon_{350}\Phi_{\text{chem}}^e$
7	356	20799	20175	0.026	526
9	362	23520	20583	0.059	1211
10	370	18071	13774	0.13	1806

^aLong-wavelength absorption maxima. ^bMolar absorptivity at the absorption maxima. ^cMolar absorptivity at 350 nm. ^dQuantum yields for the disappearance of starting materials upon irradiation at 350 nm. ^eProduct of the photolysis quantum yield and molar absorptivity.

shorter wavelength, from 370 nm for **10** to 356 and 362 nm for **7** and **9**, respectively, indicating that like the Bhc group azacoumarin-based protecting groups can be cleaved under uncaging light conditions (330–385 nm). The molar absorptivities at 350 nm of **7** ($\epsilon = 20175 \text{ M}^{-1} \text{ cm}^{-1}$) and **9** ($\epsilon = 20583 \text{ M}^{-1} \text{ cm}^{-1}$) are higher than that of **10**. The photolysis quantum yields for disappearance of starting materials were calculated from the single decay curves using the equation $\Phi = 1/(I \times 10^3 \epsilon t_{90})$ as reported by Tsien.¹⁷ The quantum yields of disappearance were determined as 0.026 for **7** and 0.059 for **9**, respectively, which are 2–5 times lower than that of **10** (0.13) possibly due to the relatively strong fluorescence of the 8-azacoumarin chromophore.¹⁸ An important factor in the development of new photolabile protecting groups is photolysis efficiency. The photolysis efficiency of caged compounds is evaluated with the product of the photolysis quantum yield (Φ_{chem}) and molar absorptivity (ϵ) and allows quantitative comparison of the overall efficiency of a photolysis reaction.¹⁹ The $\epsilon_{350}\Phi_{\text{chem}}$ values of **7** and **9** are 526 and 1211, respectively, and that of **10** is 1806. The observed $\epsilon_{350}\Phi_{\text{chem}}$ values of 8-azacoumarin derivatives **7** and **9** were sufficiently high to support practical applications to caging chemistry. Taking into account the excellent aqueous solubility of the 8-azacoumarin chromophore, 8-azacoumarin-based

photolabile protecting groups promise to be useful for caging chemistry.

In conclusion, we have designed and performed a simple and robust strategy for increasing the hydrophilicity of coumarin chromophores based on the concept of structural isosterism of amides and enols. Replacement of the C7–C8 enol double bond of the Bhc group with a polar and hydrophilic amide bond led to the development of novel 8-azacoumarin-type protecting groups, which can be removed photolytically and which showed markedly enhanced hydrophilicity and high photolysis efficiency supporting applications to caging chemistry. These studies provide the basis for future work including the development of novel hydrophilic molecules, to which it is difficult by standard approaches to introduce additional hydrophilic functionalities. Current efforts are aimed at expanding this strategy to other caging groups and functional molecules, which will offer highly effective methods for spatial and temporal control of biological activities.

■ ASSOCIATED CONTENT

Supporting Information

Experimental detail, synthesis, and characterization data. This material is available free of charge via the Internet at <http://pubs.acs.org>.

■ AUTHOR INFORMATION

Corresponding Author

*E-mail: tamamura.mr@tmd.ac.jp.

Present Address

[§]Department of Applied Chemistry and Biochemical Engineering, Faculty of Engineering, Shizuoka University, Hamamatsu, Shizuoka 432-8561, Japan.

Author Contributions

[#]T.N and H.T. contributed equally to this work.

Notes

The authors declare no competing financial interest.

■ ACKNOWLEDGMENTS

This research was supported by the Naito Foundation (Natural Science Scholarship) and in part by a Grant-in-Aid for Young Scientist (B) from the Ministry of Education, Culture, Sports, Science and Technology. We are grateful to Dr. Tomoya Hirano (Tokyo Medical and Dental University: TMDU) for assistance in the measurement of photophysical properties and to Chiaki Kambe (TMDU) for preliminary experiments.

■ REFERENCES

- (1) (a) Pillai, V. N. R. *Synthesis* **1980**, 1–26. (b) Binkley, R. W.; Flechtner, T. W. In *Synthetic Organic Photochemistry*; Horspool, W. M., Ed.; Plenum: New York, 1984; pp 375–423. (c) Pillai, V. N. R. *Organic Photochemistry*; Padwa, A., Ed.; Marcel Dekker: New York, 1987; Vol. 9, pp 225–323. (d) Bochet, C. G. *J. Chem. Soc., Perkin Trans. 1* **2002**, 125–142. (e) Bochet, C. G.; Blanc, A. In *CRC Handbook of Organic Photochemistry and Photobiology*; Griesbeck, A., Oelgemöller, M., Ghetti, F., Eds.; CRC: Boca Raton, 2012; Vol. 1, pp 73–93. (f) Klán, P.; Šolomek, T.; Bochet, C. G.; Blanc, A.; Givens, R.; Rubina, M.; Popik, V.; Kostikov, A.; Wirz, J. *Chem. Rev.* **2013**, *113*, 119–191.
- (2) (a) Adams, S. R.; Tsien, R. Y. *Annu. Rev. Physiol.* **1993**, *55*, 755–784. (b) Curley, K.; Lawrence, D. S. *Pharmacol. Ther.* **1999**, *82*, 347–354. (c) Dorman, G.; Prestwich, G. D. *Trends Biotechnol.* **2000**, *18*,

- 64–77. (d) Shigeri, Y.; Tatsu, Y.; Yumoto, N. *Pharmacol. Ther.* **2001**, *91*, 85–92.
- (3) (a) Caged Compounds. In *Methods in Enzymology*; Marriot, G., Ed.; Academic Press: New York, 1998; Vol. 291. (b) Mayer, G.; Heckel, A. *Angew. Chem., Int. Ed.* **2006**, *45*, 4900–4921. (c) Ellis-Davies, G. C. R. *Nat. Methods* **2007**, *4*, 619–628. (d) Lee, H. M.; Larson, D. R.; Lawrence, D. S. *ACS Chem. Biol.* **2009**, *4*, 409–427.
- (4) Nitrobenzyl-type: (a) Engels, J.; Schlaeger, E.-J. *J. Med. Chem.* **1977**, *20*, 907–911. (b) Kaplan, J. H.; Forbush, B., III; Hoffman, J. F. *Biochemistry* **1978**, *17*, 1929–1935.
- (5) Benzoin-type: (a) Sheehan, J. C.; Wilson, R. M. *J. Am. Chem. Soc.* **1964**, *86*, 5277–5281. (b) Givens, R. S.; Athey, P. S.; Kueper, L. W., III; Matuszewski, B.; Xue, J. *J. Am. Chem. Soc.* **1992**, *114*, 8708–8710. (c) Hansen, K. C.; Rock, R. S.; Larsen, R. W.; Chan, S. I. *J. Am. Chem. Soc.* **2000**, *122*, 11567–11568.
- (6) Phenacyl-type: (a) Sheehan, J. C.; Umezawa, K. *J. Org. Chem.* **1973**, *38*, 3771–3774. (b) Givens, R. S.; Weber, J. F. W.; Jung, A. H.; Park, C.-H. *Methods Enzymol.* **1998**, *291*, 1–29. (c) Conrad, P. G., II; Givens, R. S.; Weber, J. F. W.; Kandler, K. *Org. Lett.* **2000**, *2*, 1545–1547.
- (7) Coumarin-type: (a) Givens, R. S.; Matuszewski, B. *J. Am. Chem. Soc.* **1984**, *106*, 6860–6861. (b) Furuta, T.; Torigai, H.; Sugimoto, M.; Iwamura, M. *J. Org. Chem.* **1995**, *60*, 3953–3956. (c) Furuta, T.; Iwamura, M. *Methods Enzymol.* **1998**, *291*, 50–63. (d) Furuta, T.; Wang, S. S. H.; Dantzker, J. L.; Dore, T. M.; Bybee, W. J.; Callaway, E. M.; Denk, W.; Tsien, R. Y. *Proc. Natl. Acad. Sci. U.S.A.* **1999**, *96*, 1193–1200. (e) Hagen, V.; Bendig, J.; Fring, S.; Eckardt, T.; Helm, S.; Reuter, D.; Kaupp, U. B. *Angew. Chem., Int. Ed.* **2001**, *40*, 1045–1048. (f) Eckardt, T.; Hagen, V.; Schade, B.; Schmidt, R.; Schweitzer, C.; Bendig, J. *J. Org. Chem.* **2002**, *67*, 703–710. (g) Geisler, D.; Kresse, W.; Wiesner, B.; Bendig, J.; Kettenmann, H.; Hagen, V. *ChemBioChem* **2003**, *4*, 162–170. (h) Nomura, W.; Narumi, T.; Ohashi, N.; Serizawa, Y.; Lewin, N. E.; Blumberg, P. M.; Furuta, T.; Tamamura, H. *ChemBioChem* **2011**, *12*, 535–539.
- (8) Hagen, V.; Dekowski, B.; Nache, V.; Schmidt, R.; Geissler, D.; Lorenz, D.; Eichhorst, J.; Keller, S.; Kaneko, H.; Benndorf, K.; Wiesner, B. *Angew. Chem., Int. Ed.* **2005**, *44*, 7887–7891.
- (9) Hagen, V.; Kilic, F.; Schaal, J.; Dekowski, B.; Schmidt, V. R.; Kotzur, N. *J. Org. Chem.* **2010**, *75*, 2790–2797.
- (10) Olson, J. P.; Kwon, H.-B.; Takasaki, K. T.; Chiu, C. Q.; Higley, M. J.; Sabatini, B. L.; Ellis-Davies, G. C. R. *J. Am. Chem. Soc.* **2013**, *135*, 5954–5957.
- (11) (a) Kim, B. H.; Venkatsean, N. *Curr. Med Chem.* **2002**, *9*, 2243–2270. (b) Meanwell, N. A. *J. Med. Chem.* **2011**, *54*, 2529–2591.
- (12) For some examples of unsubstituted alkene dipeptide isosteres, see: (a) Jenkins, C. L.; Vasbinder, M. M.; Miller, S. J.; Raines, R. T. *Org. Lett.* **2005**, *7*, 2619–2622. (d) Wiktelius, D.; Luthman, K. *Org. Biomol. Chem.* **2007**, *5*, 603–605. (e) Badur, N. G.; Harms, K.; Koert, U. *Synlett* **2007**, *1*, 99–102 and references therein.
- (13) (a) Namanja, A.; Wang, X. J.; Xu, B.; Mercedes-Camacho, A. Y.; Wilson, B. D.; Wilson, K. A.; Etkorn, F. A.; Peng, J. W. *J. Am. Chem. Soc.* **2010**, *132*, 5607–5609. (b) Tamamura, H.; Hiramatsu, K.; Ueda, S.; Wang, Z.; Kusano, S.; Terakubo, S.; Trent, J. O.; Peiper, S. C.; Yamamoto, N.; Nakashima, H.; Otaka, A.; Fujii, N. *J. Med. Chem.* **2005**, *48*, 380–391. (c) Narumi, T.; Hayashi, R.; Tomita, K.; Kobayashi, K.; Tanahara, N.; Ohno, H.; Naio, T.; Kodama, E.; Matsuoka, M.; Oishi, S.; Fujii, N. *Org. Biomol. Chem.* **2010**, *8*, 616–621 and references therein.
- (14) Yavari, I.; Adib, M.; Hojabri, L. *Tetrahedron* **2002**, *58*, 6895–6899.
- (15) Furuta, T.; Takeuchi, H.; Isozaki, M.; Takahashi, Y.; Kanehara, M.; Sugimoto, M.; Watanabe, T.; Noguchi, K.; Dore, T. M.; Kurahashi, T.; Iwamura, M.; Tsien, R. Y. *ChemBioChem* **2004**, *5*, 1119–1128.
- (16) HPLC monitoring of the hydrolysis stability in PBS of azacoumarins revealed that compound 7 was more resistant than the parent Bhc 10. See Supporting Information for details.
- (17) Tsien, R. Y.; Zuker, R. S. *Biophys. J.* **1986**, *50*, 843–853.
- (18) The quantum yields of fluorescence were determined as 0.39 for 7 and 0.29 for 9, respectively.
- (19) Brown, E. B.; Shear, J. B.; Adams, S. R.; Tsien, R. Y.; Webb, W. W. *Biophys. J.* **1999**, *76*, 489–499.

Imidazolium Salt-Catalyzed Friedel–Crafts-Type Conjugate Addition of Indoles: Analysis of Indole/Imidazolium Complex by High Level *ab Initio* Calculations

Tetsuo Narumi,^[a] Seiji Tsuzuki,^[b] and Hirokazu Tamamura*^[a]

Abstract: We describe the facile synthesis of 3-substituted indoles by Friedel–Crafts-type conjugate addition catalyzed by imidazolium salts. The reactions proceed under mild conditions with no base, solvent, or N-heterocyclic carbene. Mechanistic studies suggest the potential mechanism operates through the dual activation of indoles involving cation– π interactions

of imidazolium cations with indoles and Lewis base activation by chloride anions derived from the imidazolium salts. High-level *ab initio* molecular orbital calculations reveal that there is a strong attraction between the imidazolium cation and the indole, and that the electrostatic and induction interactions strongly contributes to the attraction in the indole/imidazolium

complex, which is a characteristic feature of the cation– π interaction.

Keywords: *ab initio* calculations · cation– π interactions · Friedel–Crafts reaction · imidazolium salts · indoles

Introduction

The cation– π interaction is a fundamental noncovalent interaction between cationic species and electron-rich π -electron systems.^[1] The interactions of cationic species, such as inorganic ions, protonated amines, or quaternary ammonium salts, with a side chain of phenylalanine, tyrosine, or tryptophan contribute strongly to biomolecular functions, such as structural stabilization of proteins and molecular recognition.^[2] Artificial systems for cation– π interactions including cyclophane molecules have been extensively studied in supramolecular and host-guest chemistry to establish the importance of the cation– π interaction.^[1a,3] Amongst such systems, small molecular artificial cation– π complexes find great utility in synthetic organic chemistry, as those

systems can provide potentially intriguing strategies towards reaction design.^[4–7] A representative example was reported by Yamada and Morita in 2002,^[4] in which an intramolecular cation– π interaction between a pyridinium cation and a benzyl moiety allows a face-selective nucleophilic addition to pyridinium salts to provide chiral 1,4-dihydropyridines. Later, Ishihara and Fushimi identified the first Cu²⁺-based artificial metalloenzyme that is effective for the enantioselective Diels–Alder and Mukaiyama–Michael reactions,^[5] in which the intramolecular cation– π interaction between the Cu²⁺ ion and the electron-rich aryl group is responsible for the transition-state assembly. In 2010, Jacobsen and co-workers reported an elegant organocatalytic system for enantioselective cationic polycyclization catalyzed by thiourea derivatives with a polycyclic aromatic group,^[6] which plays a critical role for the stabilization of cation– π interactions in the transition state to achieve high levels of enantioselectivity. Furthermore, the importance of potential cation– π interactions in various organocatalytic reactions has been proposed.^[7]

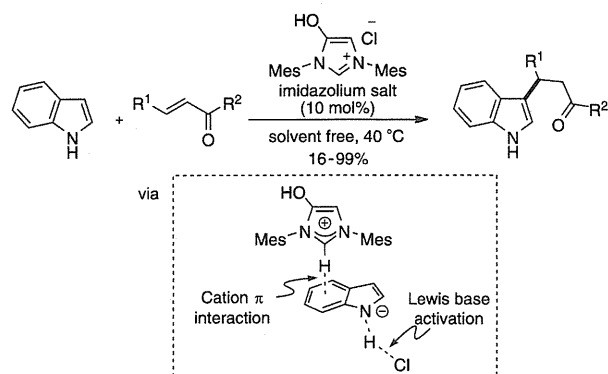
In this report, we document a remodeling of intermolecular cation– π interactions of imidazolium cations with indoles, which can trigger Friedel–Crafts-type conjugate additions^[8] of indoles that proceed under mild conditions to provide various 3-substituted indoles (Scheme 1). Preliminary data suggest that the potential mechanism operates through the dual activation of indoles by a cation– π interaction with imidazolium cations and Lewis base activation by chloride anions derived from the imidazolium salts. High-level *ab initio* molecular orbital calculations support the presence of a cation– π interaction in the indole/imidazolium complex.

[a] Dr. T. Narumi,⁺ Prof. Dr. H. Tamamura
Institute of Biomaterials and Bioengineering
Tokyo Medical and Dental University
Chiyoda-ku, Tokyo 101-0062 (Japan)
Fax: (+81)3-5280-8039
E-mail: tamamura.mr@tmd.ac.jp

[b] Dr. S. Tsuzuki
Research Initiative of Computational Sciences (RICS)
Nanosystem Research Institute
National Institute of Advanced Industrial Science and Technology
(AIST)
Tsukuba, Ibaraki 305-8565 (Japan)

[⁺] Current address:
Department of Applied Chemistry and Biochemical Engineering
Faculty of Engineering, Shizuoka University
3-5-1 Johoku, Hamamatsu 432-8561 (Japan)

Supporting information for this article is available on the WWW under <http://dx.doi.org/10.1002/ajoc.201400026>.



Scheme 1. Imidazolium-salt-catalyzed Friedel-Crafts-type conjugate addition through the dual activation of indole. Mes = mesityl.

Results and Discussion

Our interest in the application of imidazolium salts emerged from N-heterocyclic carbene (NHC) catalysts. Recently, considerable efforts have been made in the development of NHC catalysis, as exemplified by benzoin and Stetter reactions, homoenolate additions, and various annulation reactions of acyl azolium intermediates.^[9] In contrast to these reactions, imidazolium salt-derived NHCs can also work as catalysts in Brønsted base activation. Movassaghi and Schmidt^[10] reported NHC-catalyzed amidation of unactivated esters with amino alcohols via the hydrogen-bonding interaction of NHCs with alcohols, which is supported by the X-ray structure of the carbene/alcohol complex. Subsequently, Scheidt and co-workers^[11] reported that the NHC (IMes) derived from IMesCl (**1a**) can effectively catalyze intermolecular conjugate additions of alcohols to activated alkenes, and Kang and Zhao^[12] reported related reactions with anilines. Consideration of such reports prompted us to invoke the NHC/indole complex as a possible generated intermediate, capable of facilitating the conjugate addition of indole **2** to the conjugated acceptors.

Chalcone **3** was used as a conjugate acceptor, and while use of **1a** as a precatalyst followed by deprotonation by *n*BuLi/LiCl provided no product (Table 1, entry 1), the use of organic bases such as Et₃N, diisopropylethylamine (DIPEA), pyridine, and 1,8-diazabicyclo[5.4.0]undec-7-ene (DBU) generated the desired product **4a** in low conversion (Table 1, entries 2–5). Upon further investigation of precatalysts, solvents and bases,^[13] we discovered the unique potential of imidazolium salts. In the absence of base, the reaction catalyzed by only IMesCl gave **4a** in moderate yield (Table 1, entry 6). It is also notable that the reaction under neat conditions proceeded smoothly in a higher yield (Table 1, entry 7).^[14]

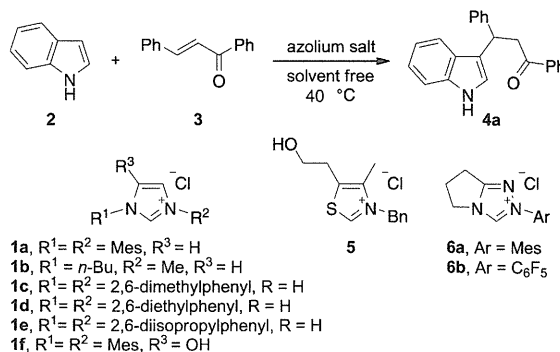
As examples of NHC catalysis requiring no base are scarce,^[15] we examined Friedel-Crafts-type conjugate additions catalyzed by azolium salts (Table 2). The choice of azolium salts was critical. Various imidazolium salts **1a–f** are effective catalysts, and the reactions provide the desired product **4a** in low to good yields (Table 2, entries 1–7),

Table 1. Optimization of the reaction conditions.

Entry	Conditions (mol %) ^[a]	Conv. [%] ^[b]
1	1a (5), <i>n</i> BuLi (5), LiCl, toluene	nr
2	1a , Et ₃ N, CH ₂ Cl ₂	trace
3	1a , DIPEA, CH ₂ Cl ₂	7
4	1a , pyridine, CH ₂ Cl ₂	8
5	1a , DBU, CH ₂ Cl ₂	24
6	1a , no base, CH ₂ Cl ₂	44
7	1a , no base, solvent-free	70

[a] Unless otherwise noted, all reactions were carried out with chalcone **3** (0.20 mmol), indole **2** (0.60 mmol, 3.0 equiv.) and IMesCl **1a** (0.02 mmol, 10 mol %) in CH₂Cl₂ (1.0 mL) at 40 °C. [b] Determined by ¹H NMR. nr = no reaction. Mes = 2,4,6-trimethylphenyl.

Table 2. Azolium salt screening for Friedel-Crafts-type conjugate additions of indoles.



Entry	Salts	Yield [%] ^[b]
1	1a	25
2	1b	9
3	1c	30
4	1d	36
5	1e	11
6	1f	72
7 ^[c]	1f	97
8	5	nr
9	6a	nr
10	6b	nr
11	NH ₄ Cl	2
12	BnMe ₃ NCl	nr
13	Me ₄ NCl	nr
14	<i>n</i> Bu ₄ NCl	nr

[a] Unless otherwise noted, all reactions were carried out with chalcone **3** (0.20 mmol), indole (**2**, 0.40 mmol, 2.0 equiv.) and azolium salt (0.02 mmol, 10 mol %) in solvent-free conditions at 40 °C for 12 h. [b] Yield of isolated product. [c] 24 h. nr = no reaction.

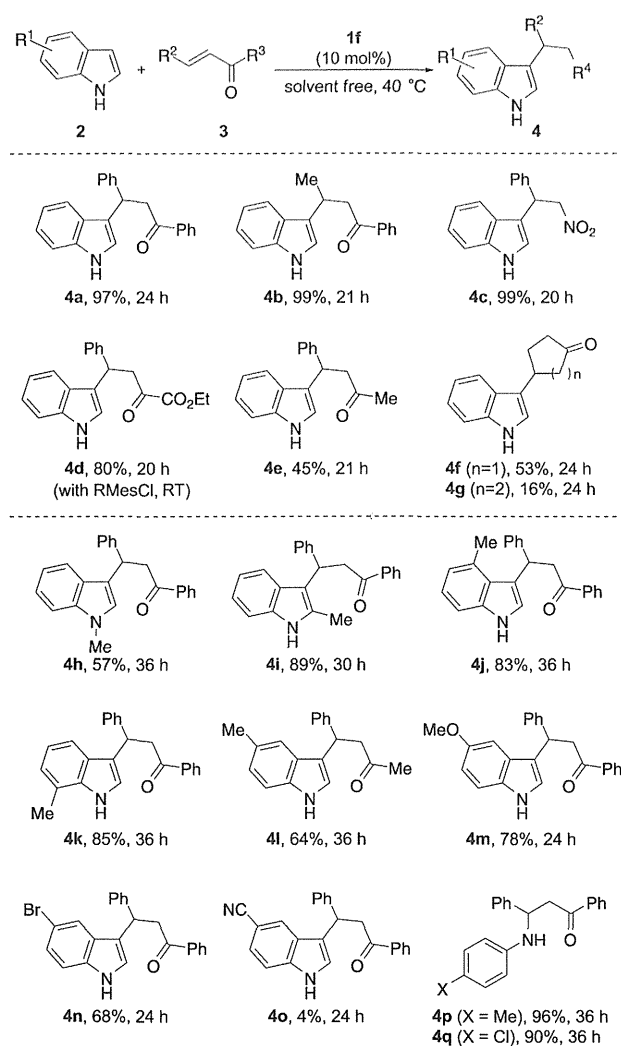
whereas a thiazolium salt **5** or triazolium salts **6** proved to be unproductive (Table 2, entries 8–10). The reaction catalyzed by ionic liquid [bmim]Cl (**1b**), which is known to be effective in the aza-Michael reaction of amines via hydrogen-bonding interactions,^[14a] produced **4a** in lower yield than other imidazolium salts with N-aryl substituents, which

suggests the importance of N-aryl substituents of imidazolium salts on the reaction, and the possibility of a different reaction pathway. Furthermore, NH_4Cl and tetraalkylammonium salts were not effective (Table 2, entries 11–14), which indicates that the core structure of imidazolium salts is critical for the reaction. The best result was obtained with 4-hydroxyimidazolium salt **1f**^[16] (HyMesCl), which was reported by Lavigne and co-workers, which gave the desired compound **4a** in 72% isolated yield (Table 2, entry 6). Finally, we found the optimized conditions: treatment of **3** (1.0 equiv.) with **2** (2.0 equiv.), and HyMesCl **1f** (10 mol%) at 40 °C for 24 h provided **4a** in quantitative yield (Table 2, entry 7).

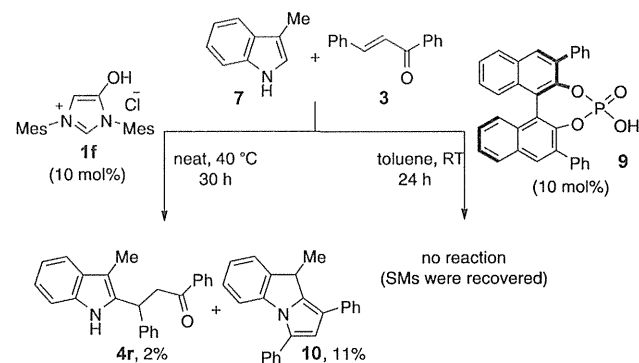
With the optimized condition in hand, we investigated a variety of conjugate acceptors interacting with indole (Scheme 2). The reactions with reactive substrates such as 1-phenylbutenone or β -nitrostyrene afforded the corresponding compounds **4b** and **4c**, respectively, in excellent yields, but the reaction with a highly reactive ketoester was sluggish and provided the desired compound **4d** in low

yield. The sluggish reactivity of the ketoester was overcome by the use of RMeCl (**6a**), and the reaction provided **4d** in 80% yield. Replacement of the phenyl ring on the ketone with an electron-donating methyl group led to a decrease in the reactivity, but the corresponding compound **4e** was produced in moderate yield. The reaction with an enoate provided no product, but cyclic enones were effective and the desired compounds **4f** and **4g** were obtained in low to moderate yields.

Examination of the substrate scope with respect to Michael donors revealed that a methyl substituent was amenable at most positions of the indole except the C3 position, and the reactions afforded the corresponding compounds **4h–l** in moderate to high yields. Although the reaction with 3-methylindole (**7**) was resistant to catalysis by a phosphoric acid catalyst,^[17,18] the reaction catalyzed by imidazolium salt **1f** afforded the desired compound **4r** in 2% yield, but also the cyclized compound **10** in 10% yield. Compound **10** is presumably produced by intramolecular cyclization of **4r** followed by olefin isomerization (Scheme 3).



Scheme 2. Substrate scope of imidazolium salt catalyzed Friedel-Crafts-type conjugate addition.

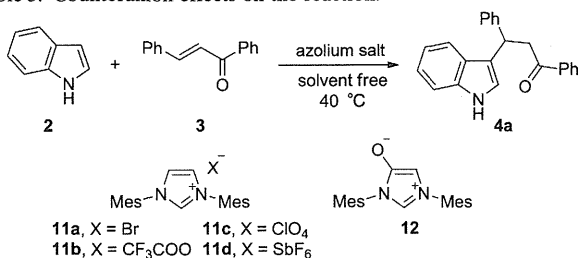


Scheme 3. Reaction with 3-methylindole.

These results demonstrate the unique nature of imidazolium salt catalysis. The reaction also tolerated an electron-donating 5-methoxy group and an electron-withdrawing 5-bromo group to produce the corresponding compounds **4m** and **4n** in 78% and 68% yield, respectively. On the other hand, the reaction of the indole substituted with a strongly electron-withdrawing 5-cyano group gave the desired indole **4o** in only 4% isolated yield. While the optimized conditions are not suited for the reactions with benzofuran and benzothiophene, aza-Michael reaction of anilines can catalyzed by **1f** to produce the corresponding compounds **4p** and **4q** in excellent yield. These results indicate the importance of a nitrogen atom in these reactions.

To gain some insight into the role played by the imidazolium salts, several mechanistic studies were performed. Counteranion studies revealed that imidazolium salts **1a**, **11a**, and **11b** with Cl^- , Br^- , and CF_3COO^- as counteranions mediate the reaction to afford **4a** in moderate conversion yields (Table 3, entries 1–3), while the use of imidazolium salts **11c** and **11d** with ClO_4^- or SbF_6^- as counteranions did not mediate the reaction (Table 3, entries 4 and

Table 3. Counteranion effects on the reaction.



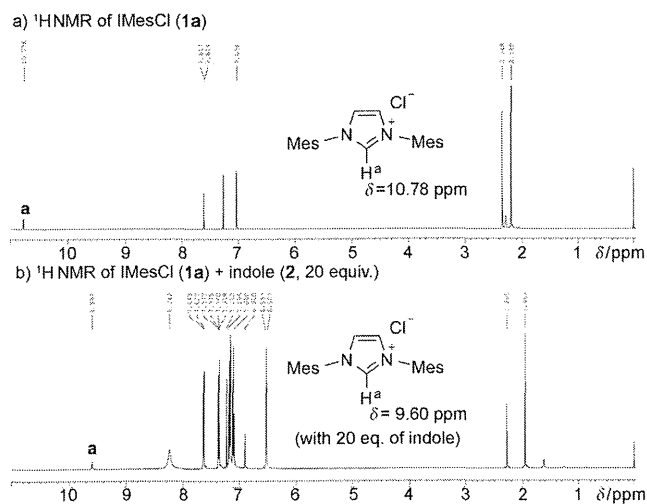
11a, X = Br
 11b, X = CF₃COO
 11c, X = ClO₄
 11d, X = SbF₆

Entry	Azolium salt	Counter anion	Conv. [%] ^[b]
1	1a	Cl ⁻	62
2	11a	Br ⁻	26
3	11b	CF ₃ COO ⁻	35
4	11c	ClO ₄ ⁻	nr
5	11d	SbF ₆ ⁻	nr
6	12	-	nr

[a] All reactions were carried out with chalcone **3** (0.20 mmol), indole (**2**, 0.40 mmol, 2.0 equiv.), and azolium salt (0.02 mmol, 10 mol%) in solvent-free conditions at 40 °C for 20 h. [b] Determined by ¹H NMR spectroscopy. nr=no reaction.

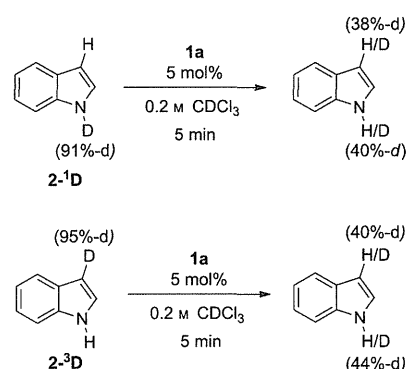
5). Furthermore, the reaction with zwitterionic imidazolium salt **12**^[16b] that lacks a counteranion failed to provide the product (Table 3, entry 6). These results indicate that the counter anion of imidazolium salts is critical for the reaction.

However, as the p*K*_a value of indole is 21.0,^[19] it would be difficult to deprotonate the N–H group of indoles with a chloride anion. At this stage, we speculated that some interactions induced by imidazolium salts could play an important role in the activation of indoles, leading to the formation of potential indole/imidazolium complexes that would enable the Friedel–Crafts-type conjugate addition. To investigate the interaction of indoles and imidazolium salts, the reaction was monitored by ¹H NMR spectroscopy. Figure 1a shows the ¹H NMR spectra of IMesCl (**1a**) in CDCl₃ (0.2 M, 20 °C) from δ = 0.00–11.0 ppm. As imidazoli-


 Figure 1. ¹H NMR investigation of the interaction of IMesCl (**1a**) and indole (**2**) in CDCl₃.

um groups are positively charged and have a relatively acidic C2 proton, imidazolium salts have been used as anion-binding receptors through the strong hydrogen bonding between the C2 proton of the imidazolium salt and various anions.^[20] Hence, the C2 proton of **1a** is shifted significantly downfield. After treatment of **1a** with 20 equivalents of indole **2**, the C2 proton of **1a** shifted significantly upfield (Δδ = 1.18 ppm, Figure 1b) while no significant shift of the other protons of imidazolium ring was detected. Moreover, small upfield shifts were detected for the protons on the mesityl groups (ca. 0.23 ppm). These results indicate that treatment of **1a** with excess indole leads to a decrease in the hydrogen-bonding interactions of the imidazolium moiety with chloride anions, and also suggests that mesityl moieties of **1a** are possibly shielded by aromatic rings.

Furthermore, deuterium labeling studies revealed that mixing a catalytic amount of **1a** and ¹D-indole **2-¹D** (91% -d) in CDCl₃ led to immediate isomerization with deuterium incorporation at the C3 position of the indole (Scheme 4), and the reaction with ³D-indole **2-³D** (95% -d) also promot-


 Scheme 4. IMesCl-catalyzed deuterium isomerization of *d*-indoles **2-¹D** and **2-³D**.

ed deuterium isomerization in a similar ratio. Also, mixing an equimolar amount of IMesCl and indole in CDCl₃ (0.2 M, 20 °C) leads rapidly to a suspension, and forms a white precipitate within 10 min (Figure 1 in the Supporting Information). These results strongly suggest that interactions of indoles with imidazolium salts are possible in the reaction media.

Details of the interactions in indole/imidazolium complex were evaluated by ab initio calculations with Gaussian 09,^[21] a powerful method for studying intermolecular interactions. Details of the computational procedures are shown in the Supporting Information.^[22] If a sufficiently large basis set is used and electron correlation is properly corrected, the calculated interaction energies agree well with the gas-phase experimental values.^[23] The cation–π interactions in the benzene complexes with alkali-metal and pyridinium cations have been studied^[1,24] and the MP2/cc-pVTZ level interaction energy potentials calculated for 16 orientations of the indole/1,3-dimethylimidazolium complex **A–P** (Figure 2) are shown in Figure 3. There is a clear tendency

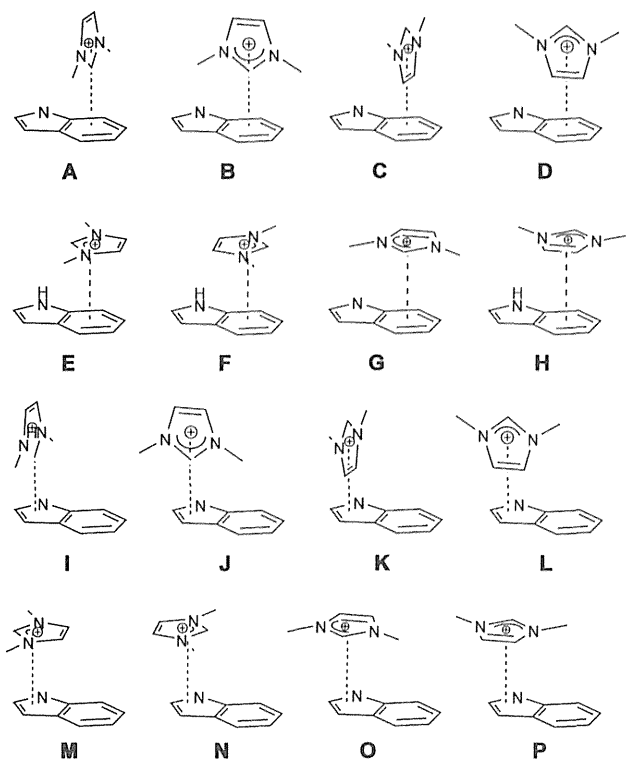


Figure 2. Geometries of indole/imidazolium complexes A–P used for calculations of interaction energy potentials.

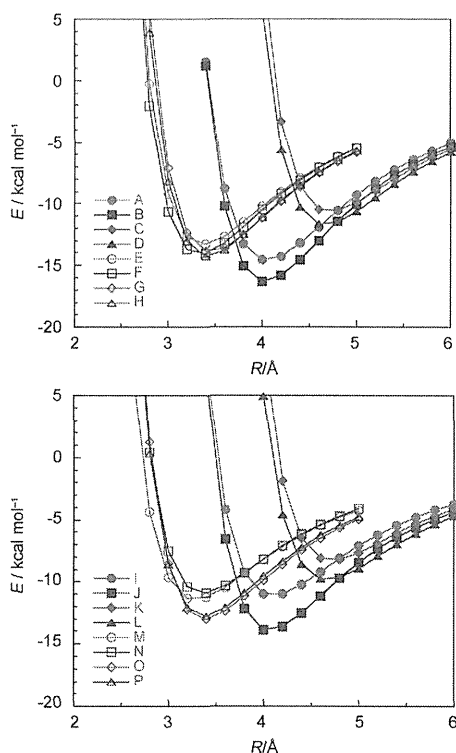


Figure 3. MP2/cc-pVTZ interaction energy potentials for indole/imidazolium complexes A–P (Figure 2). Intermolecular distance (R) is the distance between the indole plane and the midpoint of the two nitrogen atoms of imidazolium.

for the interaction energy for the geometries A–H, in which the imidazolium ring locates above the six-membered ring of indole, to be larger than in the corresponding geometries I–P, in which the imidazolium ring is located above the five-membered ring of indole, which indicates that 1,3-dimethylimidazolium cation prefers to interact with the six-membered ring of indole. These results are consistent with the optimized structure for the indole/ Na^+ complex, in which the sodium cation is positioned on the six-membered ring of indole.^[1,25] Interestingly, the interaction energy in the complexes (A, B, I, and J), in which the C2–H bond of the imidazolium ion points toward the indole, is larger than that of the corresponding complexes (C, D, K, and L), in which the C4–H and C5–H bonds of imidazolium have contact with the indole. In particular, the T-shaped structure B has a very large interaction energy compared with those of the other structures.

Two stable geometries were obtained by geometry optimization of the indole/1,3-dimethylimidazolium complex. The optimized geometries and the related interaction energies (E_{int} , the CCSD(T) level total interaction energy at the basis set limit) are shown in Figure 4. Both structures are T-

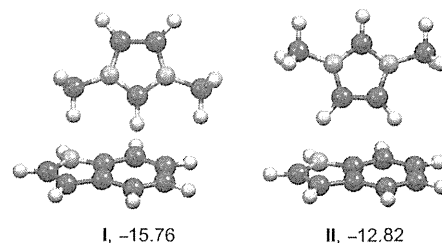


Figure 4. Optimized geometries and CCSD(T) interaction energies at the basis set limit (kcal mol^{-1}) for an indole/1,3-dimethylimidazolium complex.

shaped. Structure I ($-15.76 \text{ kcal mol}^{-1}$) in which the C₂–H bond of imidazolium points toward the center of six-membered ring of indole is more stable than II ($-12.82 \text{ kcal mol}^{-1}$) in which the C₄–H and C₅–H bonds of the imidazolium ion have contact with the indole. The larger electrostatic and induction interactions in I compared with II (Table 4) are the origin of the greater stability of the geometry I. The center of the positive charge distributions of imidazolium ring is close to the midpoint between the two nitrogen atoms of the imidazolium ring.^[26] The shorter distance between the midpoint and the indole plane in geometry I is apparently the cause of the larger electrostatic and induction energies.

Calculated interaction energies for the complex are compared with those for the benzene complexes with pyridinium and K^+ cations in Table 4. The E_{int} for the most stable form (I) is larger than that of the benzene/pyridinium complex ($-14.77 \text{ kcal mol}^{-1}$) and also close to that of the benzene/ K^+ complex ($-17.2 \text{ kcal mol}^{-1}$), which indicates that strong attraction that exists between an indole and a 1,3-di-

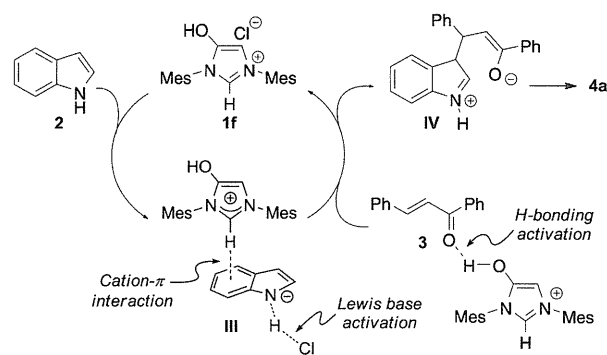
Table 4. Electrostatic, induction, and dispersion energies of indole/1,3-dimethylimidazolium and other cation/ π complexes.^[a]

	$E_{\text{HF}}^{[b]}$	$E_{\text{int}}^{[c]}$	$E_{\text{es}}^{[d]}$	$E_{\text{ind}}^{[e]}$	$E_{\text{shot}}^{[f]}$	$E_{\text{corr}}^{[g]}$
I	-8.70	-15.76	-8.86	-6.57	6.73	-7.06
II	-5.82	-12.82	-7.45	-5.19	6.82	-7.01
benzene/pyridinium ^[h]		-14.77	-8.12	-9.13	8.12	-5.63
benzene/K ⁺ ^[h]		-17.2	-11.9	-12.8	11.8	-4.4

[a] Energy in kcal mol⁻¹. The geometries of clusters **I** and **II** are shown in Figure 4. [b] HF/aug-cc-pVTZ interaction energy. [c] Estimated CCSD(T) interaction energy at the basis set limit (ECCSD(T) limit). [d] Electrostatic energy. [e] Induction energy. [f] Repulsion energy. [g] Effect of electron correlation on the interaction energy; mainly dispersion energy. [h] Data in ref. [23].

methylimidazolium cation. The large electrostatic and induction contributions to the attraction in the indole/1,3-dimethylimidazolium complex, as in the cases of the benzene complexes with pyridinium and alkali-metal cations, show that the interactions in the indole/1,3-dimethylimidazolium complex should be categorized as a cation- π interaction.

A plausible reaction mechanism is shown in Scheme 5. Although the reaction mechanism through the imidazolium-mediated hydrogen-bonding activation of conjugate ac-



Scheme 5. Proposed reaction mechanism.

ceptors such as Brønsted acid catalysis cannot be excluded,^[14,27] based on the results of our mechanistic studies, we propose a catalytic process involving possible cation- π interactions of indole/imidazolium complexes. The cation- π interaction of imidazolium salts with indole leads to the formation of an indole/imidazolium complex (**III**). Close juxtaposition of imidazolium cations to electron-rich indole rings, which leads to the increased acidity of indoles,^[28] would facilitate a Lewis base activation of the NH group of the indole by the imidazolium salt-derived chloride anion. This is followed by Friedel-Crafts-type conjugate addition to the acceptor, presumably activated by the hydroxy group of HyMes⁺, to generate the corresponding enolate **IV**. Subsequent tautomerization of **IV** affords the 3-substituted indole **4a** and regenerates the imidazolium-salt catalyst.

Conclusions

We have described an imidazolium salt-catalyzed Friedel-Crafts-type conjugate addition of indoles that requires no base, no solvent, and no carbene to provide various 3-substituted indoles in good to excellent yields at ambient temperatures. The key to this reaction catalyzed by imidazolium salts is the unique activation of indoles prompted by the possible cation/ π interaction of indole/imidazolium complexes. High-level ab initio calculation reveals that there is a strong attraction between the indole and the 1,3-dimethylimidazolium cation, and that the most stable T-shaped structure of indole/imidazolium complex is stabilized by large electrostatic and induction interactions, which is a characteristic feature of the cation- π interaction. These findings expand the potential for the development of novel reactions based on these classes of molecules. Efforts to develop an enantioselective version^[29] of this reaction and to explore the detailed mechanism are currently in progress.

Experimental Section

General Procedure for Azolium Salt-Catalyzed Friedel-Crafts-Type Conjugate Addition of Indole **2**.

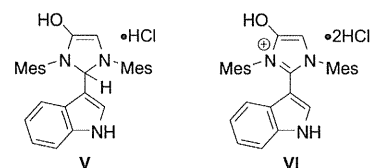
Chalcone **3** (0.50 mmol, 1.0 equiv.), indole (**2**, 2.0 equiv.), and HyMesCl (**1e**, 10 mol%) were placed in a test tube. The reaction mixture was stirred at 40 °C for 24 h. Purification by flash column chromatography on silica gel with *n*-hexane/EtOAc gave the corresponding compound **4a**.

Acknowledgements

This research was supported by a Grant-in-Aid for Scientific Research on Innovative Areas "Advanced Molecular Transformations by Organocatalysts" from The Ministry of Education, Culture, Sports, Science and Technology, Japan. We are grateful to Prof. Dr. T. Ohwada (The University of Tokyo) and Prof. Dr. S. Yamada (Ochanomizu University) for helpful discussions.

- [1] For reviews, see: a) J. C. Ma, D. A. Dougherty, *Chem. Rev.* **1997**, *97*, 1303; b) J. P. Gollivan, D. A. Dougherty, *Proc. Natl. Acad. Sci. USA* **1999**, *96*, 9459; c) N. Zacharias, D. A. Dougherty, *Trends Pharmacol. Sci.* **2002**, *23*, 281; d) D. A. Dougherty, *Acc. Chem. Res.* **2013**, *46*, 885.
- [2] For discussion of cation- π interaction in protein structures, see: a) L. Brocchieri, S. Karlin, *Proc. Natl. Acad. Sci. USA* **1994**, *91*, 9297; b) S. Karlin, M. Zuker, L. Brocchieri, *J. Mol. Biol.* **1994**, *239*, 227.
- [3] For reviews, see: a) H.-J. Schneider, *Chem. Soc. Rev.* **1994**, *23*, 227; b) N. S. Scrutton, A. R. Raine, *Biochem. J.* **1996**, *319*, 1; c) E. A. Meyer, R. K. Castellano, F. Diederich, *Angew. Chem. Int. Ed.* **2003**, *42*, 1210; *Angew. Chem.* **2003**, *115*, 1244; d) H.-J. Schneider, *Angew. Chem. Int. Ed.* **2009**, *48*, 3924; *Angew. Chem.* **2009**, *121*, 3982; e) L. M. Salonen, M. Ellermann, F. Diederich, *Angew. Chem. Int. Ed.* **2011**, *50*, 4808; *Angew. Chem.* **2011**, *123*, 4908.
- [4] S. Yamada, C. Morita, *J. Am. Chem. Soc.* **2002**, *124*, 8184.
- [5] K. Ishihara, M. Fushimi, *Org. Lett.* **2006**, *8*, 1921.
- [6] a) R. R. Knowles, S. Lin, E. N. Jacobsen, *J. Am. Chem. Soc.* **2010**, *132*, 5030; b) C. Uyeda, E. N. Jacobsen, *J. Am. Chem. Soc.* **2011**, *133*, 5062. For a recent review of noncovalent interactions, see:

- R. R. Knowles, E. N. Jacobsen, *Proc. Natl. Acad. Sci. USA* **2010**, *107*, 20678.
- [7] For examples of organocatalysis involving possible cation- π interactions, see: a) D. L. Comins, S. P. Joseph, R. R. Goehring, *J. Am. Chem. Soc.* **1994**, *116*, 4719; b) T. Kawabata, M. Nagato, K. Takasu, K. Fuji, *J. Am. Chem. Soc.* **1997**, *119*, 3169; c) S. J. Miller, G. T. Copeland, N. Papaioannou, T. E. Horstmann, E. M. Ruel, *J. Am. Chem. Soc.* **1998**, *120*, 1629; d) K. A. Ahrendt, C. J. Borths, D. W. C. MacMillan, *J. Am. Chem. Soc.* **2000**, *122*, 4243; e) V. B. Birman, E. W. Uffman, J. Hui, X. M. Li, C. J. Kilbane, *J. Am. Chem. Soc.* **2004**, *126*, 12226; S. M. Mennen, J. T. Blank, M. B. Tran-Dube, J. E. Imbriglio, S. J. Miller, *Chem. Commun.* **2005**, 195; f) B. Hu, M. Meng, Z. Wang, W. Du, J. S. Fossey, X. Hu, W.-P. Deng, *J. Am. Chem. Soc.* **2010**, *132*, 17041. For a recent review, see: S. Yamada, J. S. Fossey, *Org. Biomol. Chem.* **2011**, *9*, 7257.
- [8] For recent reviews of organocatalytic Friedel-Crafts reactions, see: a) V. Terrasson, R. M. de Figueiredo, J. M. Campagne, *Eur. J. Org. Chem.* **2010**, 2635; b) M. Rueping, B. J. Nachtsheim, *Beilstein J. Org. Chem.* **2010**, *6*, 6; c) S.-L. You, Q. Cai, M. Zeng, *Chem. Soc. Rev.* **2009**, *38*, 2190.
- [9] For reviews, see: a) J. M. Moore, T. Rovis in *Topics in Current Chemistry, Vol. 291* (Ed.: B. List), Springer, Berlin, **2009**, pp. 77–144; b) D. Enders, O. Niemeier, A. Henseler, *Chem. Rev.* **2007**, *107*, 5606; c) K. Zeitler, *Angew. Chem. Int. Ed.* **2005**, *44*, 7506; *Angew. Chem.* **2005**, *117*, 7674; d) D. Enders, T. Balensiefer, *Acc. Chem. Res.* **2004**, *37*, 534; e) P.-C. Chiang, J. W. Bode in *N-Heterocyclic Carbenes: From Laboratory Curiosities to Efficient Synthetic Tools* (Ed.: S. Díez-Conzález), Royal Society of Chemistry, Cambridge, **2010**, pp. 399–435.
- [10] M. Movassaghi, M. A. Schmidt, *Org. Lett.* **2005**, *7*, 2453.
- [11] E. M. Phillips, M. Riedrich, K. A. Scheidt, *J. Am. Chem. Soc.* **2010**, *132*, 13179.
- [12] Q. Kang, Y. Zhang, *Org. Biomol. Chem.* **2011**, *9*, 6715.
- [13] See the Supporting Information for details.
- [14] For a similar reaction of thiols with enones catalyzed by an ionic liquid via hydrogen-bonding interactions with the C2 hydrogen atom of imidazolium ions, see: A. Sarkar, S. R. Roy, A. K. Chakraborti, *Chem. Commun.* **2011**, *47*, 4538. For several transformations mediated by azolium ions as acid catalysts, see: a) V. Jurcik, R. Wilhelm, *Tetrahedron: Asymmetry* **2006**, *17*, 801; b) A. K. Chakraborti, S. R. Roy, *J. Am. Chem. Soc.* **2009**, *131*, 6902; c) P. V. G. Reddy, S. Tabassum, A. Blanrue, R. Wilhelm, *Chem. Commun.* **2009**, *45*, 5910; d) S. R. Roy, A. K. Chakraborti, *Org. Lett.* **2010**, *12*, 3866; e) L. Myles, R. Gore, M. Špulák, N. Gathergood, S. J. Connon, *Green Chem.* **2010**, *12*, 1157; f) A. Sarkar, S. R. Roy, N. Parikh, A. K. Chakraborti, *J. Org. Chem.* **2011**, *76*, 7132; g) L. Myles, N. Gathergood, S. J. Connon, *Chem. Commun.* **2013**, *49*, 5316.
- [15] a) J. Kaeobamrung, J. Mahatthanachai, P. Zheng, J. W. Bode, *J. Am. Chem. Soc.* **2010**, *132*, 8810; b) J. Mahatthanachai, J. Kaeobamrung, J. W. Bode, *ACS Catal.* **2012**, *2*, 494.
- [16] For the synthesis of HyMesCl **1f**, see: a) L. Benhamou, V. César, H. Gornitzka, N. Lugan, G. Lavigne, *Chem. Commun.* **2009**, 4720; b) L. Benhamou, N. Vujkovic, V. César, H. Gornitzka, N. Lugan, G. Lavigne, *Organometallics* **2010**, *29*, 2616.
- [17] For recent reviews on chiral phosphoric acid catalysts, see: a) S. J. Connon, *Angew. Chem. Int. Ed.* **2006**, *45*, 3909; *Angew. Chem.* **2006**, *118*, 4013; b) T. Akiyama, J. Itoh, K. Fuchibe, *Adv. Synth. Catal.* **2006**, *348*, 999; c) T. Akiyama, *Chem. Rev.* **2007**, *107*, 5744; d) G. Adair, S. Mukherjee, B. List, *Aldrichimica Acta* **2008**, *41*, 31; e) M. Terada, *Chem. Commun.* **2008**, 4097; f) M. Terada, *Bull. Chem. Soc. Jpn.* **2010**, *83*, 101; g) M. Terada, *Synthesis* **2010**, 1929; h) A. Zamfir, S. Schenker, M. Freund, S. B. Tsogoeva, *Org. Biomol. Chem.* **2010**, *8*, 5262; i) M. Terada, *Curr. Org. Chem.* **2011**, *15*, 2227.
- [18] T. Sakamoto, J. Itoh, K. Mori, T. Akiyama, *Org. Biomol. Chem.* **2010**, *8*, 5448.
- [19] F. G. Bordwell, G. E. Drucker, H. E. Fried, *J. Org. Chem.* **1981**, *46*, 632.
- [20] a) E. Alcalde, C. Alvarez-Rua, S. García-Granda, E. García-Rodríguez, N. Mesquida, L. Pérez-García, *Chem. Commun.* **1999**, 295; b) E. Alcalde, N. Mesquida, L. Pérez-García, *Eur. J. Org. Chem.* **2006**, 3988; c) I. Dinarès, C. G. de Miguel, N. Masquida, E. Aldalde, *J. Org. Chem.* **2009**, *74*, 482.
- [21] Gaussian 09, Revision C.01, M. J. Frisch, et al. Gaussian, Inc., Wallingford CT, **2009**.
- [22] a) M. Head-Gordon, J. A. Pople, M. J. Frisch, *Chem. Phys. Lett.* **1988**, *153*, 503; b) J. A. Pople, M. Head-Gordon, K. Raghavachari, *J. Chem. Phys.* **1987**, *87*, 5968; c) B. J. Ransil, *J. Chem. Phys.* **1961**, *34*, 2109; d) S. F. Boys, F. Bernardi, *Mol. Phys.* **1970**, *19*, 553; e) T. Helgaker, W. Klopper, H. Koch, J. Noga, *J. Chem. Phys.* **1997**, *106*, 9639; f) S. Tsuzuki, K. Honda, T. Uchimaru, M. Mikami, K. Tanabe, *J. Am. Chem. Soc.* **2000**, *122*, 3746; g) K. Shibasaki, A. Fujii, M. Mikami, S. Tsuzuki, *J. Phys. Chem. A* **2007**, *111*, 753; h) A. J. Stone, M. Alderton, *Mol. Phys.* **1985**, *56*, 1047; i) A. J. Stone, *The theory of intermolecular forces*, Clarendon Press, Oxford, **1996**; j) A. J. Stone, A. Dullweber, M. P. Hodges, P. L. A. Popelier, D. J. Wales, *Orient: a program for studying interactions between molecules version 3.2*. University of Cambridge, **1995**; k) A. J. Stone, *J. Chem. Theory Comput.* **2005**, *1*, 1128–1132; l) A. J. Stone, *Mol. Phys.* **1985**, *56*, 1065; m) P. T. van Duijnen, M. Swart, *J. Phys. Chem. A* **1998**, *102*, 2399.
- [23] a) T. H. Dunning, Jr., *J. Phys. Chem. A* **2000**, *104*, 9062; b) S. Tsuzuki, T. Uchimaru, K. Matsumura, M. Mikami, K. Tanabe, *J. Chem. Phys.* **1999**, *110*, 11906.
- [24] S. Tsuzuki, M. Mikami, S. Yamada, *J. Am. Chem. Soc.* **2007**, *129*, 8656, and references therein.
- [25] S. Mecozzi, A. P. West, D. A. Dougherty, *Proc. Natl. Acad. Sci. USA* **1996**, *93*, 10566.
- [26] S. Tsuzuki, H. Tokuda, M. Mikami, *Phys. Chem. Chem. Phys.* **2007**, *9*, 4780.
- [27] It should be noted that although an alternative mechanism catalyzed by the Brønsted acid catalysts **V** and **VI** that might be generated from the Mannich-type reaction of indole to imidazolium would be possible, neither **V** nor **VI** were detected by ¹H NMR spectroscopy. For a discussion of imidazolium-derived ionic liquids as Brønsted acid catalysts in the presence of protic additives, such as alcohols, see ref. 14e.



- [28] Atomic charge distributions of indole were calculated by electrostatic potential fitting using Merz-Singh-Kollman Scheme from the MP2/6-311G** wavefunctions of isolated indole and an indole-dimethylimidazolium complex, indicating that a cation- π interaction in the indole/imidazolium complex largely affect the atomic charge distributions of indole, rendering the NH group of indole more cationic. See the Supporting Information for details.
- [29] Several chiral imidazolium salts with a hydroxy group for the enantioselective reaction were attempted, but no enantioselectivity was achieved. See the Supporting Information for details.

Received: January 30, 2014
Published online: March 24, 2014

Synthesis and Characterization of Quantum Dot Nanoparticles Bound to the Plant Volatile Precursor of Hydroxy-apo-10'-carotenal

Vo Anh Tu,[†] Atsushi Kaga,[†] Karl-Heinz Gericke,[‡] Naoharu Watanabe,^{†,§} Tetsuo Narumi,[†] Mitsuo Toda,[†] Bernhard Brueckner,[⊥] Susanne Baldermann,^{*,⊥,||} and Nobuyuki Mase^{*,†}

[†]Department of Applied Chemistry and Biochemical Engineering, Graduate School of Engineering, and Green Energy Research Division, Research Institute of Green Science and Technology, Shizuoka University, 3-5-1 Johoku, Hamamatsu, Shizuoka 432-8561, Japan

[‡]Institute for Physical and Theoretical Chemistry, University of Technology, Braunschweig, Hans-Sommer-Strasse 10, D-38106, Braunschweig, Germany

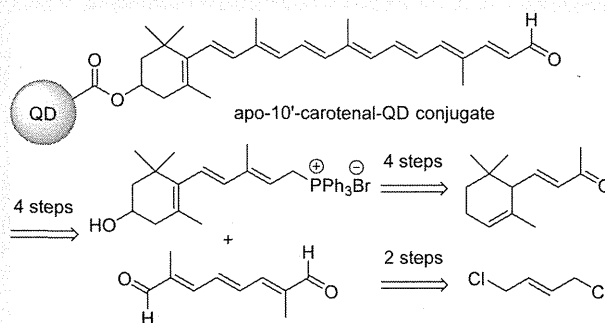
[§]Graduate School of Science and Technology, Shizuoka University, Shizuoka, 432-8561 Japan

[⊥]Leibniz-Institute of Vegetable and Ornamental Crops Großbeeren/Erfurt e.V., Theodor-Echtermeyer-Weg 1, 14979 Großbeeren, Germany

^{||}Institute of Nutritional Science, University of Potsdam, Arthur-Scheunert-Allee 114-116, 14558 Nuthetal, Germany

Supporting Information

ABSTRACT: This study is focused on the synthesis and characterization of hydroxy-apo-10'-carotenal/quantum dot (QD) conjugates aiming at the *in vivo* visualization of β -ionone, a carotenoid-derived volatile compound known for its important contribution to the flavor and aroma of many fruits, vegetables, and plants. The synthesis of nanoparticles bound to plant volatile precursors was achieved via coupling reaction of the QD to C₂₇-aldehyde which was prepared from α -ionone via 12 steps in 2.4% overall yield. The formation of the QD-conjugate was confirmed by measuring its fluorescence spectrum to observe the occurrence of fluorescence resonance energy transfer.



INTRODUCTION

Plant carotenoids are tetraterpenes with polyene chains that may contain up to 15 conjugated double bonds; therefore, they act as natural pigments and are responsible for the distinct yellow to the red-orange color of fruits, flowers, vegetables, and leaves. Further, they can be oxidized at almost every position and cleaved enzymatically at distinct double bonds. The carotenoid cleavage dioxygenase (CCD) is known to be a specific nonheme enzyme for the oxidation of the rigid backbone of carotenoids.¹ CCD exhibits a high degree of regio- and stereospecificity for the cleavage of specific double bond positions in diverse substrates. The cleavage products of CCDs play important roles in plant growth, protection against light exposure, and as chemoattractants and repellents in plants and cyanobacteria,² as anti-fungal agents, and as the source of fragrances for reproduction.³ Among these products, a total of 1700 volatile compounds have been isolated and identified from more than 90 plant families.⁴ These volatile compounds are released from leaves, flowers, and fruits into the atmosphere and from roots into the soil; they defend plants against herbivores and pathogens and provide a reproductive advantage by attracting the pollinators and seed dispersers.

β -Ionone, one of the most abundant carotenoid-derived compounds, is a significant volatile compound, which

contributes to the fragrance in the flower of *Boronia megastigma*,⁵ *Osmanthus fragrans*,⁶ *Rosa damascena*, and *Camellia sinensis*.⁷ Although its concentration is not particularly high, β -ionone is among the most potent flavor-active molecules characterized by extremely low odor thresholds. Therefore, we are interested in determining the formation pathway yielding β -ionone as a secondary metabolite *in vivo*, which has not been identified yet. We would like to propose a hypothesis that helps to visualize β -ionone *in vivo* (Figure 1). The C₂₇-apocarotenal intermediate (apo-10'-carotenal) from the first CCD4-catalyzed oxidative cleavage of C₄₀-carotenoid in the plastid is prepared for coupling to nanocrystal quantum dot (QD) to afford apocarotenal-QD conjugate 1. QD is employed for the coupling reaction owing to its unique properties such as water solubility, photostability, and exceptional fluorescence.⁸ The apocarotenal-QD conjugate 1 is prepared and subsequently administrated into the living plant cell. Conjugate 1 cleaves to β -ionone-QD conjugate 2, catalyzed by enzyme CCD1. Because of the fluorescence property of QD, β -ionone-QD conjugate 2 can be detected by two-photon microscopy, a fluorescence imaging technique allowing the imaging of living

Received: March 14, 2014

Published: July 15, 2014

